BMC Cardiovascular Disorders

RESEARCH

Open Access

Development and validation of an integrated prognostic model for all-cause mortality in heart failure: a comprehensive analysis combining clinical, electrocardiographic, and echocardiographic parameters

Yahui Li[1†], Jiayu Xu[2†], Xuhui Liu[3], Xujie Wang[4], Chunxia Zhao[1*] and Kunlun He[5*]

Abstract

Background Accurate risk prediction in heart failure remains challenging due to its complex pathophysiology. We aimed to develop and validate a comprehensive prognostic model integrating demographic, electrocardiographic, echocardiographic, and biochemical parameters.

Methods We conducted a retrospective cohort study of 445 heart failure patients. The cohort was randomly divided into training ($n=312$) and validation ($n=133$) sets. Feature selection was performed using LASSO regression followed by backward stepwise Cox regression. A nomogram was constructed based on independent predictors. Model performance was assessed through discrimination, calibration, and decision curve analyses. Random survival forest analysis was conducted to validate variable importance.

Results During a median follow-up of 4.14 years, 142 deaths (31.91%) occurred. Our model development followed a systematic approach: initial feature selection using LASSO regression identified 15 potential predictors, which were further refined to nine independent predictors through backward stepwise Cox regression. The final predictors included age, NYHA class, left ventricular systolic dysfunction, atrial septal defect, aortic valve annulus calcification, tricuspid regurgitation severity, QRS duration, T wave offset, and NT-proBNP. The integrated model demonstrated good discrimination for 2-, 3-, and 5-year mortality prediction in both training (AUCs: 0.726, 0.755, 0.809) and validation cohorts (AUCs: 0.686, 0.678, 0.706). Calibration plots and decision curve analyses confirmed the model's reliability and clinical utility across different time horizons. A nomogram was constructed for individualized risk prediction. Kaplan-Meier analyses of individual predictors revealed significant stratification of survival outcomes,

†Yahui Li and Jiayu Xu are co-first authors and contribute equally to this work.

*Correspondence:
Chunxia Zhao
zhaocx2001@126.com
Kunlun He
kunlunhe@plagh.org

Full list of author information is available at the end of the article

while restricted cubic spline analyses demonstrated non-linear relationships between continuous variables and mortality risk. Random survival forest analysis identified the top five predictors (age, NT-proBNP, QRS duration, tricuspid regurgitation severity, NYHA), which were compared with our nine-variable model, confirming the superior performance of the integrated model across all time points.

Conclusions Our integrated prognostic model showed robust performance in predicting all-cause mortality in heart failure patients. The model's ability to provide individualized risk estimates through a nomogram may facilitate clinical decision-making and patient stratification.

Clinical trial number Not applicable.

Keywords Heart failure, Prognosis, Risk prediction, Machine learning, Nomogram

Introduction

Heart failure (HF) remains a major global public health challenge, affecting approximately 64.3 million people worldwide and accounting for substantial morbidity, mortality, and healthcare costs [1–3]. The prevalence of HF continues to rise with an aging population and improved survival from other cardiovascular diseases, placing an increasing burden on healthcare systems globally [4]. Despite advances in therapeutic strategies, including novel pharmacological interventions and device therapies, the prognosis of HF patients remains poor, with 5-year mortality rates exceeding 50% in some populations [5, 6]. This high mortality rate underscores the critical need for accurate risk prediction tools to guide clinical decision-making and resource allocation.

Accurate risk stratification is crucial for optimizing patient management and resource allocation in HF care. Traditional prognostic assessments have relied heavily on individual clinical parameters, such as New York Heart Association (NYHA) functional classification, left ventricular ejection fraction, and natriuretic peptide levels [7, 8]. These parameters, while valuable, often provide only partial insights into the complex pathophysiology of HF. The multifaceted nature of HF progression, involving neurohormonal, inflammatory, and structural cardiac changes, suggests that a more comprehensive approach incorporating multiple parameters might better capture the full spectrum of disease severity and progression [9]. This comprehensive approach could potentially identify high-risk patients who might benefit from more intensive monitoring or aggressive therapeutic interventions. Electrocardiographic (ECG) parameters have emerged as valuable prognostic indicators in HF, offering insights into the electrical manifestations of cardiac dysfunction. QRS duration, T-wave characteristics, and other ECG markers reflect underlying electrical remodeling and have been consistently associated with adverse outcomes in various HF populations [10, 11]. These parameters are valuable as they are typically available from routine clinical assessments; however, some variables were not fully available in our dataset due to missing values. Similarly, echocardiographic parameters provide crucial information about cardiac structure and function, with various measurements showing independent prognostic value [12, 13]. Modern echocardiographic techniques can assess multiple aspects of cardiac function, including systolic and diastolic function, valve status, and structural remodeling. The integration of these parameters with established clinical markers and biomarkers might enhance prognostic accuracy and provide a more complete picture of cardiac dysfunction [14]. Recent studies have highlighted the potential of multimodal risk prediction models in HF. Natriuretic peptides, particularly NT-proBNP, have demonstrated strong prognostic value across different HF phenotypes and stages [15, 16], while demographic factors and clinical classifications continue to provide fundamental prognostic information that complements more sophisticated markers [17]. The combination of multiple prognostic markers has shown promise in improving risk prediction accuracy. However, most existing models focus on limited aspects of cardiac assessment or specific patient subgroups, potentially missing important prognostic information that could be derived from a more comprehensive evaluation [18, 19]. This limitation highlights the need for integrated approaches that can capture the full spectrum of HF pathophysiology.

Machine learning approaches have shown promise in improving risk prediction by capturing complex relationships between multiple variables [20, 21]. These advanced analytical methods can integrate diverse data types, including demographic characteristics, cardiac imaging parameters, biomarkers, and ECG measurements, potentially offering more accurate prognostic assessments than traditional statistical approaches [22]. The ability to handle large numbers of variables and identify non-linear relationships makes these methods particularly suited for complex diseases like HF. However, the clinical application of such models often requires rigorous validation in diverse populations and demonstration of incremental value over existing risk stratification methods [23]. The challenge lies in developing models that are both comprehensive and practical for clinical implementation.

Therefore, we aimed to develop and validate a comprehensive prognostic model for all-cause mortality in HF patients by integrating demographic characteristics, ECG parameters, echocardiographic measurements, NT-proBNP levels, and NYHA classification. This integrated approach aims to capture the multiple facets of HF pathophysiology and provide a more accurate assessment of patient risk. We hypothesized that this multimodal approach would provide superior prognostic accuracy compared to models based on individual parameters or limited variable sets, potentially offering clinicians a more reliable tool for risk stratification and treatment planning.

Methods

Study population and design

This retrospective cohort study was approved by the Institutional Review Board of the Chinese People's Liberation Army General Hospital and was conducted in accordance with the Declaration of Helsinki. We consecutively enrolled patients hospitalized for heart failure in the Department of Cardiology between October 2017 and June 2024, with all-cause mortality as the primary endpoint. Survival time was calculated from admission to death or last follow-up. Heart failure diagnosis was established according to the 2021 European Society of Cardiology (ESC) Guidelines [7]. We collected comprehensive baseline characteristics including demographics (age, gender, height, weight), lifestyle factors (smoking and drinking status), and clinical parameters (blood pressure, heart rate, NYHA functional class). All participants underwent systematic evaluations including electrocardiography, echocardiography, and biomarker assessment. The electrocardiographic examination documented cardiac electrical activity parameters including rate measurements (ventricular and atrial rates), interval durations (QRS, QT, and corrected QT by both Fredericia and Framingham methods), electrical axes (P-wave and T-wave), and specific wave measurements. Echocardiographic assessment comprised detailed structural measurements (chamber dimensions, wall thickness), functional evaluations (systolic and diastolic function), and comprehensive assessment of cardiac abnormalities including shunts, septal defects, thrombi, aneurysms, and wall motion abnormalities. Particular attention was paid to valvular conditions, documenting the presence and severity of stenosis and regurgitation across all cardiac valves, valvular calcification, and prosthetic valve status. NT-proBNP was measured as a biomarker of heart failure severity.

We selected the average value of QRS duration and other ECG parameters because this approach reduces the impact of individual abnormal beats or noise on the final results, ensuring both the stability and representativeness of the data.

To ensure the reliability and consistency of the ECG parameter extraction, two independent experts, both with extensive experience in ECG analysis, were involved in the process. Both experts were blinded to the clinical outcomes and patient identities to eliminate potential bias. The process was structured as follows: (1) Independent Review: Each expert individually reviewed the raw ECG data and manually extracted the relevant parameters (e.g., QRS duration, QTc). The experts were trained to follow a standardized protocol to ensure uniformity in their approach to data extraction. (2) Collaboration and Cross-Verification: After the initial extraction, the two experts compared their results for each patient. If there were discrepancies in the extracted parameters, the experts discussed the differences and reviewed the ECGs again to reach a consensus. This collaborative review process was conducted to ensure that the final data set accurately represented the true physiological values. (3) Discrepancy Resolution: In the event of unresolved discrepancies, a third senior expert was consulted to provide a final determination. However, the experts were able to resolve most discrepancies through discussion and further examination of the ECG traces. This rigorous review process ensured that the extracted parameters were both reliable and consistent. (4) Quality Control: To further minimize potential bias, a random sample of 10% of the ECGs was reviewed by both experts a second time after a period of time to assess the reproducibility of their results. Any differences found were addressed through re-evaluation and consensus.

The inclusion criteria were as follows

(1) age ≥ 18 years; (2) diagnosed with heart failure according to the 2021 ESC Guidelines; (3) available complete data including: Basic clinical data (demographics, NYHA classification); Standard electrocardiogram parameters; Complete echocardiography examination results; NT-proBNP level (4) available follow-up data for survival assessment. The exclusion criteria included: (1) Patients with atrial fibrillation; (2) incomplete or poor quality ECG recordings; (3) inadequate echocardiographic imaging quality; (4) missing critical clinical parameters; (5) loss to follow-up or uncertain survival status. All eligible patients were randomly divided at a 7:3 ratio into training and validation sets. The training set was used to develop prognostic models incorporating electrocardiographic and echocardiographic parameters, while the validation set was used to assess the model performance in predicting all-cause mortality. The inclusion and exclusion criteria, as well as the technical approach of this study, are depicted in Fig. 1.

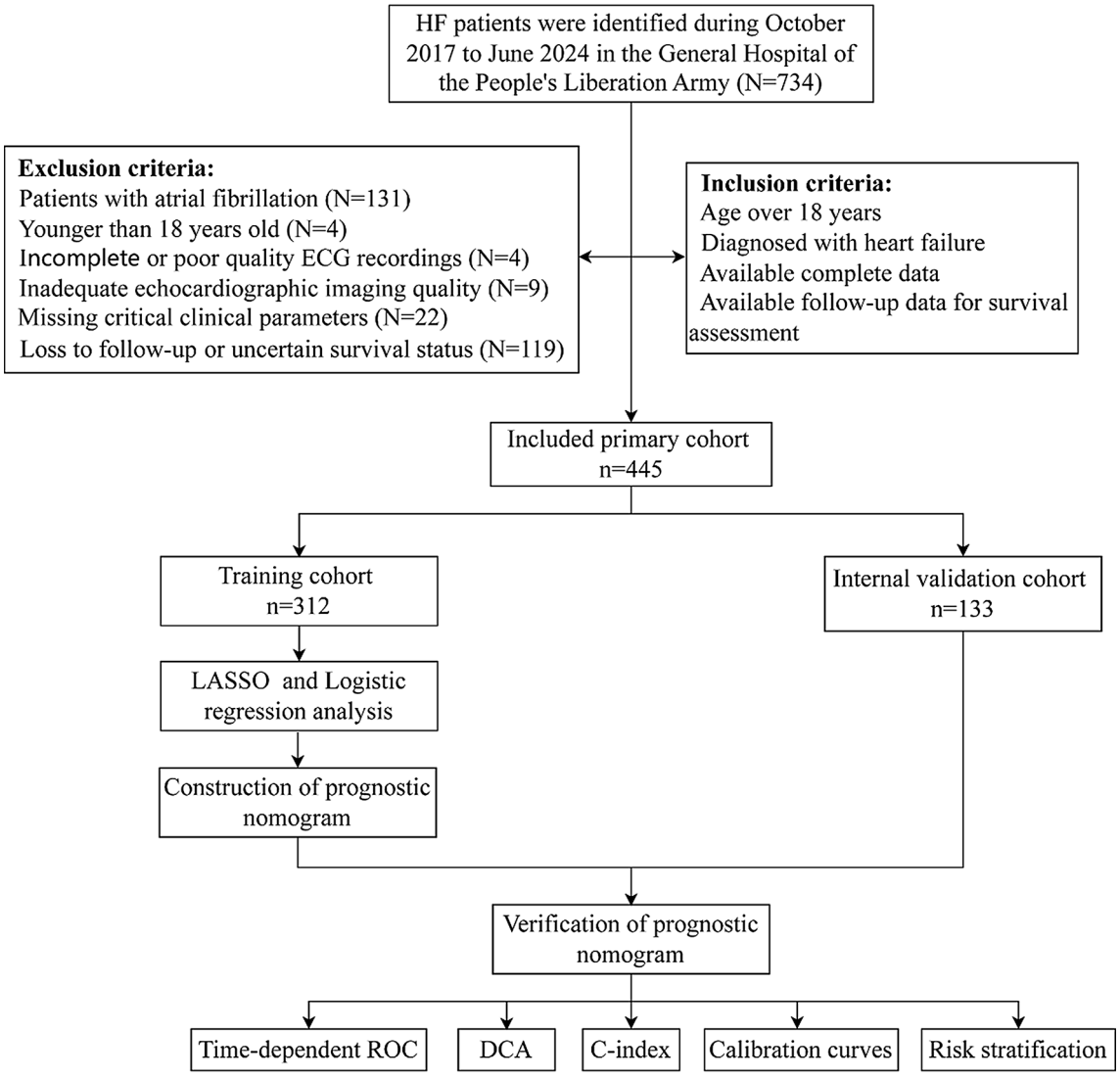

Fig. 1 Flow diagram of the selection of eligible HF patients. Abbreviation: HF: Heart failure; LASSO: Least absolute shrinkage and selection operator; ROC: Receiver operating characteristic curve; DCA: Decision curve analysis

Data preprocessing

Missing data patterns were systematically evaluated for all variables (Supplementary Fig. 2 and Supplementary Table 2). Variables with missing rates exceeding 20% were excluded from subsequent analyses. These excluded variables encompassed three main categories:

1. Left ventricular parameters: Left Ventricular End Diastolic Diameter (23.82%), Left Ventricular End Systolic Diameter (23.82%), Left Ventricular End Diastolic Volume (23.82%), Left Ventricular End Systolic Volume (23.82%), Left Ventricular Anteroposterior Diameter (77.3%);
2. Other cardiac chamber measurements: Right Atrial Maximum Diameter (24.04%), Left Atrial Transverse Diameter (23.82%), Left Atrial Superior Inferior Diameter (23.82%), Right Ventricle Ratio (29.21%), Left Ventricle (29.21%), Right Ventricular Maximum Diameter (29.66%);
3. Vascular and septal measurements: Right Pulmonary Artery Diameter (24.27%), Left Pulmonary Artery Diameter (24.27%), Aortic Sinus Superior Diameter (24.27%), Aortic Sinus Diameter (24.27%), Interventricular Septal Thickness (78.65%);
4. Electrocardiographic parameters: P-R Interval (26.74%), P Offset (26.74%), P Onset (26.74%), P Axis (26.74%).

For the remaining variables with missing rates below 20%, missing values were imputed using the Multiple Imputation by Chained Equations (MICE) algorithm with five iterations to ensure robust estimation of missing data. After completing the imputation, we checked

the imputation results using convergence plots and density curve plots. We plotted the changes in the mean and standard deviation of each variable over the iterations. When multiple lines converge and overlap, it can be considered as convergence (Supplementary Fig. 2). In the density curve plot, red represents the distribution of imputed data, and blue represents the distribution of observed data. The higher the overlap, the better (Supplementary Fig. 3). No statistical difference was observed in the baseline before and after imputation (Supplementary Table 3).

Collect clinical parameters

Electrocardiographic parameters were assessed following the 2021 AHA/ACC/HRS Guideline. Basic ECG parameters included ventricular and atrial rates. Interval measurements comprised QRS duration (measured from QRS onset to offset), QT interval (from QRS onset to T wave end), and corrected QT intervals calculated using both Fredericia's (QTc = QT/RR^1/3) and Framingham formulas. The electrical axes assessment included P wave and T wave axes, while wave characteristics encompassed QRS count, Q wave onset/offset, and T wave offset. Echocardiographic measurements were performed according to the 2015 American Society of Echocardiography and European Association of Cardiovascular Imaging recommendations. Chamber dimensions included left atrial anteroposterior diameter, left ventricular posterior wall thickness, left and right ventricular cavities, right atrial transverse diameter, and right ventricular transverse diameter. Vascular measurements comprised aortic diameter and right pulmonary artery diameter. Ventricular function was assessed through left ventricular shortening fraction, ejection fraction (EF), and evaluation of systolic and diastolic dysfunction. Structural abnormalities were documented, including the presence of shunts (at great vessel and atrial levels), atrial septal defects, apical thrombi, ventricular aneurysms, segmental wall motion abnormalities, and pericardial effusion. Valvular assessment included documentation of annular calcification (aortic and mitral), presence of prosthetic valves (aortic and mitral), and severity grading of valvular stenosis (aortic and mitral) and regurgitation (aortic, mitral, tricuspid, and pulmonary). NT-proBNP levels were measured as a biomarker of heart failure severity. Clinical characteristics included age, gender, height, weight, lifestyle factors (smoking and drinking status), blood pressure (systolic and diastolic), heart rate, and NYHA functional classification.

Statistical analysis and model development

All statistical analyses and model development were performed using R software (version 4.3.1; R Foundation for Statistical Computing, Vienna, Austria). Differences in demographic and clinical characteristics between the training and validation cohorts were compared using Mann-Whitney U test for non-normally distributed continuous variables and chi-square test for categorical variables. Statistical significance was determined using a two-tailed alpha = 0.05. Feature selection employed a two-step approach. First, the least absolute shrinkage and selection operator (LASSO) regression with 10-fold cross-validation was applied to the training cohort to identify potential predictors. Subsequently, these LASSO-selected variables underwent backward stepwise Cox regression analysis. Multicollinearity among the final selected variables was assessed using variance inflation factor (VIF). Model performance was evaluated through multiple approaches. Discrimination was assessed using time-dependent receiver operating characteristic (ROC) curves for 2-, 3-, and 5-year mortality predictions in both training and validation sets. Calibration curves were plotted to assess the agreement between predicted and observed outcomes. The clinical utility of the model was evaluated using decision curve analysis (DCA). The prognostic value of categorical variables was assessed using Kaplan-Meier survival analyses. For continuous variables, optimal cutoff values were determined using the 'survminer' package. The relationships between continuous predictors and mortality were examined using restricted cubic splines (RCS) with three knots placed at the 10th, 50th, and 90th percentiles to assess potential non-linear associations. A nomogram was constructed to provide a practical tool for individual risk prediction. Further analysis using random survival forest with 1000 trees was performed to identify the top five most important variables from our nine predictors. The optimal node size was determined through iterative testing from 1 to 75. Subsequently, comparative analyses between our nine-variable model and models constructed using these top five variables were conducted. Model comparisons included time-dependent ROC curves, calibration plots, and decision curve analyses at 2-, 3-, and 5-year time points in both training and validation cohorts.

Result

Patient characteristics and outcomes

Baseline demographic and clinical characteristics of the total cohort ($N = 445$) are detailed in Supplementary Table 1. The median age was 63.98 years (IQR: 52.58–72.84), with a male predominance (68.31%). Lifestyle factors revealed that 47.41% of patients had smoking history (27.19% current smokers, 20.22% former smokers) and 37.97% reported alcohol consumption. Electrocardiographic evaluation demonstrated a median ventricular rate of 80.00 beats/min (IQR: 68.00–92.00), QRS duration of 98.00 ms (IQR: 86.00-110.00), and QT interval of 400.00 ms (IQR: 368.00-430.00). Comprehensive

echocardiographic assessment revealed multiple cardiac abnormalities. The median ejection fraction was 45.00% (IQR: 35.00–56.00), with systolic and diastolic dysfunction observed in 9.66% and 24.94% of patients, respectively. Cardiac chamber measurements showed left atrial cavity enlargement in 46.52% of patients and right atrial cavity enlargement in 23.37%. The majority of patients (93.48%) presented with valvular regurgitation, distributed across tricuspid (mild: 58.65%, moderate: 13.71%, severe: 4.72%), mitral (mild: 53.93%, moderate: 16.85%, severe: 5.17%), and aortic valves (mild: 35.96%, moderate: 8.99%, severe: 2.02%). Additional structural findings included segmental wall motion abnormalities (26.52%), pericardial effusion (13.71%), valvular annulus calcification (6.52%), and ventricular aneurysm (5.62%). The median NT-proBNP level was 2.94×10^3 pg/mL (IQR: 1.05–8.89). For the main analysis, patients were randomly divided into training ($n = 312$) and validation ($n = 133$) cohorts, with baseline characteristics presented in Table 1. During a median follow-up of 4.14 years (IQR: 2.57–4.68), 142 deaths (31.91%) occurred. The majority of baseline characteristics showed no significant differences between the two cohorts, including age, gender, cardiovascular risk factors, cardiac structural parameters, and NT-proBNP levels (all $p > 0.05$). Only NYHA functional classification ($p = 0.037$) and several electrocardiographic parameters including ventricular rate ($p = 0.023$), atrial rate ($p = 0.017$), and QRS count ($p = 0.021$) showed significant differences between the groups, suggesting overall comparable baseline characteristics between the training and validation cohorts.

Feature selection using LASSO regression

LASSO regression with 10-fold cross-validation was performed to select potential predictors from the training cohort. Supplementary Fig. 4 illustrates the feature selection process using LASSO regression. The optimal lambda value was determined to be 0.043 through cross-validation (Supplementary Fig. 4A). The coefficient variation curve demonstrates how variables were selected with increasing penalty (Supplementary Fig. 4B). At this optimal lambda value, 15 variables were selected and their relative contributions are visualized in Supplementary Table 4. Aortic valve annulus calcification and left ventricular systolic dysfunction showed the strongest positive associations (coefficients: 0.473 and 0.455, respectively), followed by tricuspid regurgitation severity and NYHA classification (coefficients: 0.197 and 0.164, respectively). Moderate associations were observed for age, right pulmonary artery diameter, NT-proBNP level, and atrial septal defect (coefficients ranging from 0.010 to 0.020). Several variables including intracardiac shunts, QRS duration, and right ventricular diameter showed weaker associations (coefficients < 0.010), while smoking status was the only variable with a negative coefficient (-0.009). Detailed coefficients of all selected variables are presented in Supplementary Table 4.

Multivariable Cox regression analysis in training cohort

The 15 variables identified by LASSO regression were further refined through backward stepwise Cox regression analysis. Multivariate analysis identified nine independent predictors of all-cause mortality (Table 2). Structural cardiac abnormalities emerged as the strongest predictors, with atrial septal defect (HR: 3.783, 95% CI: 0.886–16.14), aortic valve annulus calcification (HR: 2.124, 95% CI: 1.076–4.192, $P = 0.030$), and left ventricular systolic dysfunction (HR: 2.031, 95% CI: 1.136–3.631, $P = 0.017$) showing the highest hazard ratios. Tricuspid regurgitation severity was also significantly associated with mortality (HR: 1.360, 95% CI: 1.044–1.773, $P = 0.023$). Among clinical parameters, age (HR: 1.034, 95% CI: 1.017–1.050, $P < 0.001$) and NT-proBNP level (HR: 1.027 per 1000 pg/mL increase, 95% CI: 1.007–1.048, $P = 0.009$) were significant predictors. Electrocardiographic parameters including QRS duration showed modest but significant associations (HR: 1.010, 95% CI: 1.003–1.018, $P = 0.009$) (Table 2). Variance inflation factor analysis confirmed the absence of significant multicollinearity among these predictors, with all VIF values below 1.25 (Supplementary Table 5).

Model performance assessment

The discriminative ability of the model was evaluated using time-dependent receiver operating characteristic (ROC) curves for 2-, 3-, and 5-year mortality predictions (Fig. 2). In the training cohort, the model demonstrated good discrimination with AUCs of 0.726 (95% CI: 0.648–0.805), 0.755 (95% CI: 0.691–0.820), and 0.809 (95% CI: 0.737–0.881) for 2-, 3-, and 5-year mortality, respectively (Fig. 2A). These findings were validated in the validation cohort, which showed AUCs of 0.686 (95% CI: 0.585–0.787), 0.678 (95% CI: 0.582–0.774), and 0.706 (95% CI: 0.547–0.866) for the corresponding time points (Fig. 2B). The overall C-index was 0.720 (95% CI: 0.665–0.775) in the training set and 0.649 (95% CI: 0.569–0.729) in the validation set. Time-dependent AUC trends are presented in Supplementary Fig. 5, showing consistent discriminative performance across different follow-up periods.

Model calibration assessment

The model's calibration was evaluated through calibration plots comparing predicted versus observed survival probabilities at 2-, 3-, and 5-year time points (Fig. 3). In the training cohort (Fig. 3A), the calibration curves for all three time points closely followed the 45-degree diagonal line, indicating good agreement between predicted and

Table 1 Baseline characteristics of the training and validation cohorts

	[ALL] *N* = 445	Train *N* = 312	Test *N* = 133	*P* value
Death				0.178
No	303 (68.09%)	219 (70.19%)	84 (63.16%)	
Yes	142 (31.91%)	93 (29.81%)	49 (36.84%)	
Gender				0.936
Female	141(31.69%)	98(31.41%)	43(32.33%)	
Male	304(68.31%)	214(68.59%)	90(67.67%)	
Smoke				0.700
Never smoker	234 (52.58%)	165 (52.88%)	69 (51.88%)	
Former smoker	121(27.19%)	87(27.88%)	34(25.56%)	
Current smoker	90(20.22%)	60(19.23%)	30(22.56%)	
Drink				0.279
Non-drinker	276 (62.02%)	200 (64.10%)	76 (57.14%)	
Occasional drinker	115 (25.84%)	74 (23.72%)	41 (30.83%)	
Regular drinker	54 (12.13%)	38 (12.18%)	16 (12.03%)	
NYHA				0.037
II	155 (34.83%)	119 (38.14%)	36 (27.07%)	
III	216 (48.54%)	148 (47.44%)	68 (51.13%)	
IV	74 (16.63%)	45 (14.42%)	29 (21.80%)	
VHD				1.000
No	386 (86.74%)	271 (86.86%)	115 (86.47%)	
Yes	59 (13.26%)	41 (13.14%)	18 (13.53%)	
Presence of shunt				0.109
No	438 (98.43%)	305 (97.76%)	133 (100.00%)	
Yes	7 (1.57%)	7 (2.24%)	0 (0.00%)	
Shunt at great vessel level left to right				0.328
No	440 (98.88%)	307 (98.40%)	133 (100.00%)	
Yes	5 (1.12%)	5 (1.60%)	0 (0.00%)	
Shunt at atrial level left to right				0.328
No	440 (98.88%)	307 (98.40%)	133 (100.00%)	
Yes	5 (1.12%)	5 (1.60%)	0 (0.00%)	
Segmental wall motion abnormality				1.000
No	327 (73.48%)	229 (73.40%)	98 (73.68%)	
Yes	118 (26.52%)	83 (26.60%)	35 (26.32%)	
Pericardial effusion				0.059
No	384 (86.29%)	276 (88.46%)	108 (81.20%)	
Yes	61 (13.71%)	36 (11.54%)	25 (18.80%)	
Left ventricular diastolic dysfunction				0.688
No	334 (75.06%)	232 (74.36%)	102 (76.69%)	
Yes	111 (24.94%)	80 (25.64%)	31 (23.31%)	
Left ventricular systolic dysfunction				0.636
No	402 (90.34%)	280 (89.74%)	122 (91.73%)	
Yes	43 (9.66%)	32 (10.26%)	11 (8.27%)	
Left ventricular cavity				0.905
No	375 (84.27%)	262 (83.97%)	113 (84.96%)	
Yes	70 (15.73%)	50 (16.03%)	20 (15.04%)	
Right ventricular cavity				0.886
No	388 (87.19%)	273 (87.50%)	115 (86.47%)	
Yes	57 (12.81%)	39 (12.50%)	18 (13.53%)	
Left atrial cavity				0.242
No	238 (53.48%)	173 (55.45%)	65 (48.87%)	
Yes	207 (46.52%)	139 (44.55%)	68 (51.13%)	
Right atrial cavity				0.116

Table 1 (continued)

	[ALL] *N* = 445	Train *N* = 312	Test *N* = 133	*P* value
No	341 (76.63%)	246 (78.85%)	95 (71.43%)	
Yes	104 (23.37%)	66 (21.15%)	38 (28.57%)	
Atrial septal defect				0.558
No	442 (99.33%)	309 (99.04%)	133 (100.00%)	
Yes	3 (0.67%)	3 (0.96%)	0 (0.00%)	
Apical thrombus				0.290
No	436 (97.98%)	304 (97.44%)	132 (99.25%)	
Yes	9 (2.02%)	8 (2.56%)	1 (0.75%)	
Ventricular aneurysm				0.990
No	420 (94.38%)	295 (94.55%)	125 (93.98%)	
Yes	25 (5.62%)	17 (5.45%)	8 (6.02%)	
Valve annulus calcification				0.944
No	416 (93.48%)	291 (93.27%)	125 (93.98%)	
Yes	29 (6.52%)	21 (6.73%)	8 (6.02%)	
Aortic valve annulus calcification				1.000
No	417 (93.71%)	292 (93.59%)	125 (93.98%)	
Yes	28 (6.29%)	20 (6.41%)	8 (6.02%)	
Mitral valve annulus calcification				0.680
No	438 (98.43%)	306 (98.08%)	132 (99.25%)	
Yes	7 (1.57%)	6 (1.92%)	1 (0.75%)	
Prosthetic valve				1.000
No	433 (97.30%)	303 (97.12%)	130 (97.74%)	
Yes	12 (2.70%)	9 (2.88%)	3 (2.26%)	
Aortic prosthetic valve				0.674
No	439 (98.65%)	307 (98.40%)	132 (99.25%)	
Yes	6 (1.35%)	5 (1.60%)	1 (0.75%)	
Mitral prosthetic valve				1.000
No	436 (97.98%)	305 (97.76%)	131 (98.50%)	
Yes	9 (2.02%)	7 (2.24%)	2 (1.50%)	
Presence of stenosis				0.770
No	422 (94.83%)	297 (95.19%)	125 (93.98%)	
Yes	23 (5.17%)	15 (4.81%)	8 (6.02%)	
Aortic valve stenosis severity				0.209
0	433 (97.30%)	305 (97.76%)	128 (96.24%)	
1	6 (1.35%)	3 (0.96%)	3 (2.26%)	
2	3 (0.67%)	1 (0.32%)	2 (1.50%)	
3	3 (0.67%)	3 (0.96%)	0 (0.00%)	
Mitral valve stenosis severity				0.169
0	429 (96.40%)	302 (96.79%)	127 (95.49%)	
1	12 (2.70%)	9 (2.88%)	3 (2.26%)	
2	2 (0.45%)	1 (0.32%)	1 (0.75%)	
3	2 (0.45%)	0 (0.00%)	2 (1.50%)	
Presence of regurgitation				0.944
No	29 (6.52%)	21 (6.73%)	8 (6.02%)	
Yes	416 (93.48%)	291 (93.27%)	125 (93.98%)	
Aortic regurgitation severity				0.585
0	236 (53.03%)	168 (53.85%)	68 (51.13%)	
1	160 (35.96%)	108 (34.62%)	52 (39.10%)	
2	40 (8.99%)	28 (8.97%)	12 (9.02%)	
3	9 (2.02%)	8 (2.56%)	1 (0.75%)	
Mitral regurgitation severity				0.093
0	107 (24.04%)	84 (26.92%)	23 (17.29%)	

Table 1 (continued)

	[ALL] *N* = 445	Train *N* = 312	Test *N* = 133	*P* value
1	240 (53.93%)	162 (51.92%)	78 (58.65%)	
2	75 (16.85%)	53 (16.99%)	22 (16.54%)	
3	23 (5.17%)	13 (4.17%)	10 (7.52%)	
Tricuspid regurgitation severity				0.642
0	102 (22.92%)	76 (24.36%)	26 (19.55%)	
1	261 (58.65%)	182 (58.33%)	79 (59.40%)	
2	61 (13.71%)	40 (12.82%)	21 (15.79%)	
3	21 (4.72%)	14 (4.49%)	7 (5.26%)	
Pulmonary regurgitation severity				0.590
0	254 (57.08%)	175 (56.09%)	79 (59.40%)	
1	163 (36.63%)	118 (37.82%)	45 (33.83%)	
2	22 (4.94%)	16 (5.13%)	6 (4.51%)	
3	6 (1.35%)	3 (0.96%)	3 (2.26%)	
Left ventricular wall thickness status				0.879
No	378 (84.94%)	264 (84.62%)	114 (85.71%)	
Yes	67 (15.06%)	48 (15.38%)	19 (14.29%)	
Interventricular septal thickness status				0.214
No	442 (99.33%)	311 (99.68%)	131 (98.50%)	
Yes	3 (0.67%)	1 (0.32%)	2 (1.50%)	
Pulmonary artery mean pressure				0.874
No	365 (82.02%)	257 (82.37%)	108 (81.20%)	
Yes	80 (17.98%)	55 (17.63%)	25 (18.80%)	
Diastolic dysfunction				0.688
No	334 (75.06%)	232 (74.36%)	102 (76.69%)	
Yes	111 (24.94%)	80 (25.64%)	31 (23.31%)	
Systolic dysfunction				0.636
No	402 (90.34%)	280 (89.74%)	122 (91.73%)	
Yes	43 (9.66%)	32 (10.26%)	11 (8.27%)	
Ventricular rate(bpm)	80.00 [68.00;92.00]	79.00 [66.00;91.00]	83.00 [71.00;95.00]	0.023
Atrial rate(bpm)	79.00 [69.00;92.00]	79.00 [67.00;90.25]	79.00 [73.00;100.00]	0.017
QRS Duration(ms)	98.00 [86.00;110.00]	98.00 [86.00;108.25]	96.00 [86.00;112.00]	0.926
QT Interval(ms)	400.00[368.00;430.00]	402.00[370.00;432.50]	400.00[362.00;426.00]	0.107
QTc Calculation(ms)	461.00[435.00;484.00]	460.00[434.75;482.00]	465.00[435.00;488.00]	0.389
QRS Count	13.00 [11.00;15.00]	13.00 [11.00;15.00]	14.00 [12.00;16.00]	0.021
Q Onset(ms)	217.00[213.00;220.00]	217.00[213.00;220.00]	217.00[213.00;221.00]	0.626
Q Offset(ms)	265.00[262.00;270.00]	265.00[262.00;270.00]	265.00[261.00;271.00]	0.858
T Offset(ms)	417.00[402.00;433.00]	418.00[404.00;435.00]	416.00[398.00;429.00]	0.143
QTc Fredericia(ms)	437.00[416.00;461.00]	438.00[417.00;461.00]	436.00[413.00;460.00]	0.609
QTc Framingham(ms)	437.00[416.00;459.00]	437.00[417.00;459.25]	435.00[415.00;458.00]	0.473
Age(years)	63.98 [52.58;72.84]	64.09 [52.30;73.03]	63.35 [53.05;72.60]	0.662
SBP(mmHg)	131.00[116.00;145.00]	130.00[115.00;143.00]	133.00[117.00;148.00]	0.352
DBP(mmHg)	75.00[67.00;86.00]	75.00[67.00;85.00]	77.00[67.00;88.00]	0.501
HR(bpm)	79.00[71.00;93.00]	79.00[70.00;91.25]	80.00[72.00;96.00]	0.241
EF(%)	45.00[35.00;56.00]	45.00[35.00;57.00]	44.00[35.00;56.00]	0.616
Aortic diameter(mm)	32.00[30.00;35.00]	32.00[30.00;35.00]	32.00[30.00;35.00]	0.698
Left atrial anteroposterior diameter(mm)	42.00[39.00;46.00]	42.00[39.00;46.00]	42.00[39.00;46.00]	0.488
Left ventricular posterior wall thickness(mm)	11.00[10.00;11.00]	11.00[10.00;11.00]	11.00[10.00;11.00]	0.643
Right atrial diameter transverse(mm)	38.00[34.00;43.00]	38.00[33.00;42.00]	38.00[34.00;45.00]	0.173
Right ventricular diameter transverse(mm)	35.00[32.00;40.00]	35.00[32.00;39.00]	36.00[33.00;41.00]	0.445
Left ventricular shortening fraction(mm)	24.00[18.00;30.00]	24.00[18.00;30.00]	24.00[18.00;29.00]	0.653
Right pulmonary artery diameter(mm)	12.00[11.00;13.00]	12.00[11.00;13.00]	12.00[11.00;13.00]	0.410

Table 1 (continued)

	[ALL] *N* = 445	Train *N* = 312	Test *N* = 133	*P* value
BMI(kg/m^2)	24.97[22.47;27.68]	24.89[22.53;27.56]	25.25[22.47;27.82]	0.604
NT-proBNP/1000(pg/mL/1000)	2.94[1.05;8.89]	2.81[0.98;8.41]	3.37[1.49;10.96]	0.104

Median: The middle value of the dataset when arranged in ascending order

IQR: Interquartile Range, the range between the 1st quartile (Q_1) and the 3rd quartile (Q_3) of the dataset

n: Frequency, the count of occurrences of a particular value

%: Percentage, the proportion of a particular value relative to the total sample size

Abbreviation: NYHA: New York Heart Association; VHD: Valvular heart disease; SBP: Systolic blood pressure; DBP: Diastolic blood pressure; HR: Heart rate; EF: Ejection fraction; BMI: body mass index; NT-proBNP: N-terminal pro-brain natriuretic peptide

Table 2 Multivariate Cox regression analysis of variables associated with All-cause mortality

Characteristics	β	SE	HR	CI	Z	*P*
NYHA	0.251	0.157	1.285	0.944–1.75	1.595	0.111
Left ventricular systolic dysfunction	0.708	0.296	2.031	1.136–3.631	2.389	0.017
Atrial septal defect	1.331	0.74	3.783	0.886–16.147	1.797	0.072
Aortic valve annulus calcification	0.753	0.347	2.124	1.076–4.192	2.171	0.03
Tricuspid regurgitation severity	0.308	0.135	1.36	1.044–1.773	2.276	0.023
QRS Duration	0.01	0.004	1.01	1.003–1.018	2.628	0.009
T Offset	-0.006	0.004	0.994	0.986–1.002	-1.441	0.149
Age	0.033	0.008	1.034	1.017–1.05	4.017	0
NT-proBNP/1000	0.027	0.01	1.027	1.007–1.048	2.618	0.009

Abbreviation: NYHA: New York Heart Association; NT-proBNP: N-terminal pro-brain natriuretic peptide

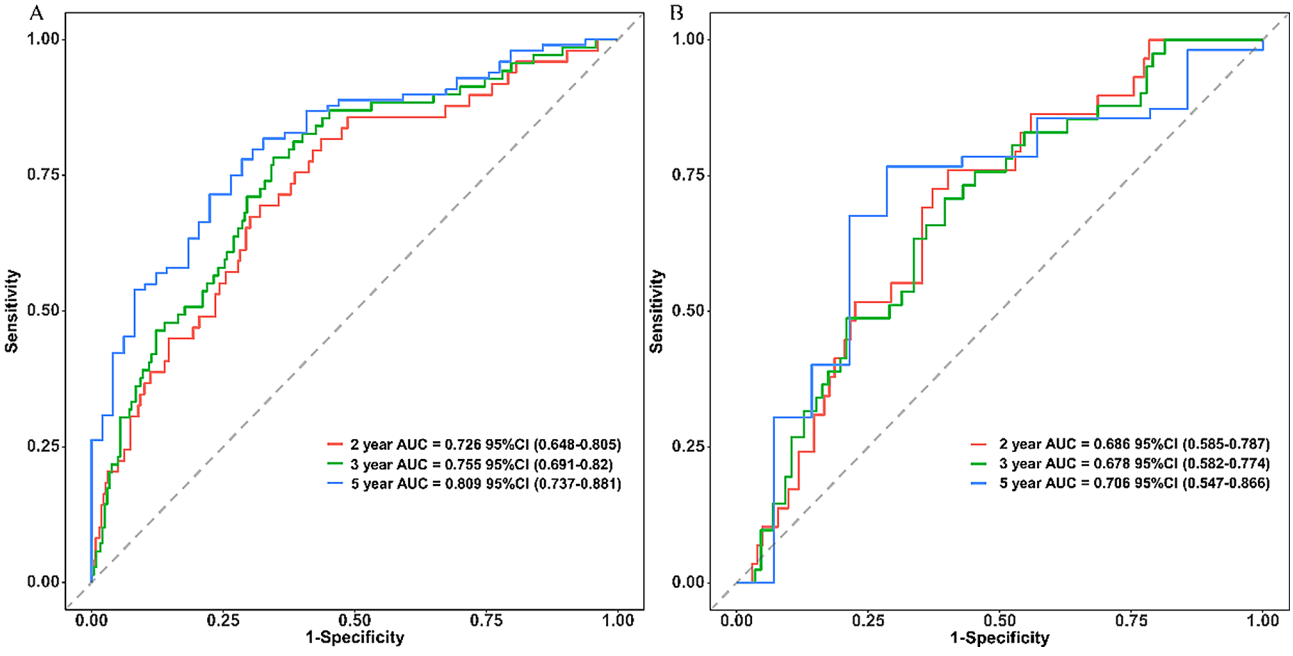

Fig. 2 Time-dependent ROC Curves for Mortality Prediction. (**A**) Training cohort. (**B**) Validation cohort

observed survival probabilities. The validation cohort (Fig. 3B) demonstrated satisfactory calibration, particularly for 2- and 3-year predictions, though with slightly wider confidence intervals due to the smaller sample size. The 5-year predictions showed some deviation in the middle range of predicted probabilities but maintained reasonable calibration at both ends of the prediction spectrum.

Clinical decision curve analysis

Decision curve analysis was performed to evaluate the clinical utility of the prediction model at different time points (Fig. 4). In the training cohort, the model showed

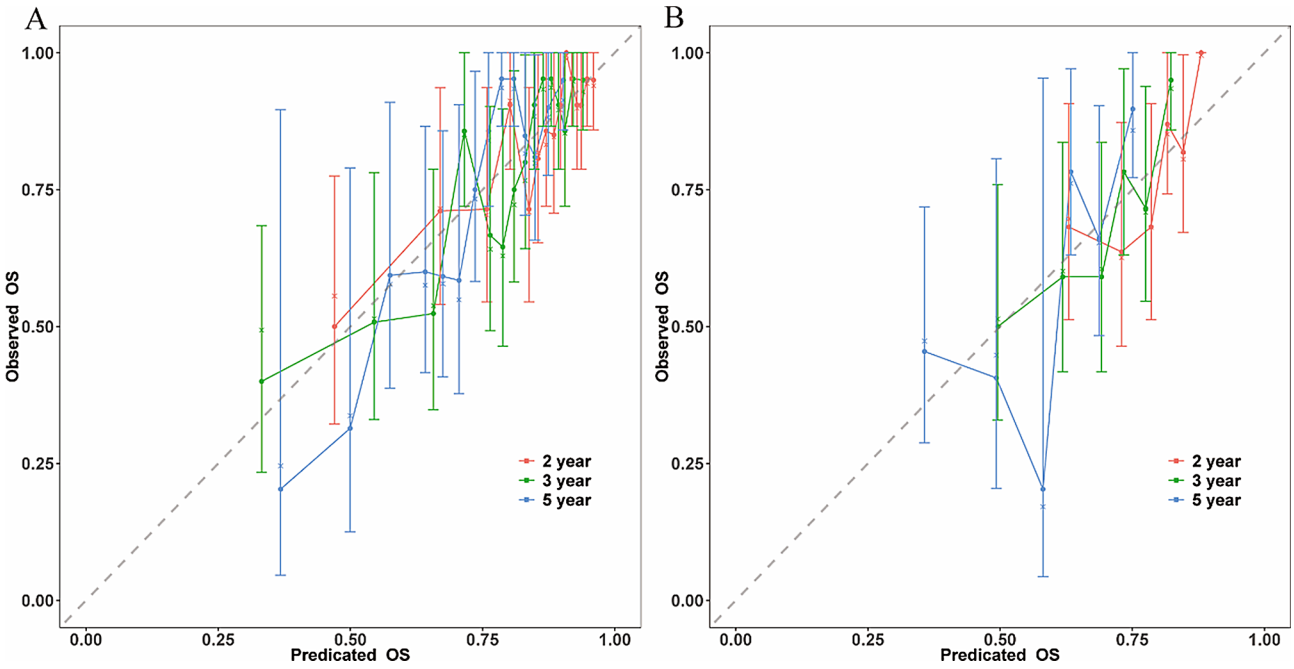

Fig. 3 Calibration Curves for 2-, 3-, and 5-year Survival Predictions. (**A**) Training cohort. (**B**) Validation cohort. The diagonal dashed lines represent perfect calibration. Error bars indicate 95% confidence intervals

consistent net benefit across various threshold probabilities at 2-year (Fig. 4A), 3-year (Fig. 4C), and 5-year (Fig. 4E) follow-up, outperforming both "treat all" and "treat none" strategies within a reasonable range of threshold probabilities (approximately 0.1 to 0.6). The validation cohort demonstrated similar patterns of net benefit at 2-year (Fig. 4B), 3-year (Fig. 4D), and 5-year (Fig. 4F) time points, though with slightly lower magnitude of benefit compared to the training cohort. The model maintained positive net benefit across a wide range of threshold probabilities, suggesting its potential clinical value in guiding treatment decisions.

Construction of a prediction nomogram in training cohort

Based on the multivariate Cox regression analysis, a nomogram was constructed to predict 2-, 3-, and 5-year survival probabilities (Fig. 5). The nomogram incorporated nine independent predictors: NYHA class (0–20 points), left ventricular systolic dysfunction (0–29 points), atrial septal defect (0–54 points), aortic valve annulus calcification (0–30 points), tricuspid regurgitation severity (0–37 points), QRS duration (0–58 points), T wave offset (0–44 points), age (0-100 points), and NT-proBNP level (0–38 points). Total points were calculated by summing the points assigned to each predictor, with a range of 0-280 points. The corresponding 2-, 3-, and 5-year survival probabilities could be estimated based on the total points, with higher total points indicating worse survival. For example, a total point score of 122 corresponded to a 2-year survival probability of 0.90, while a score of 247 indicated a 2-year survival probability of 0.10. Similar interpretations could be made for 3-year (range: 105–230 points) and 5-year (range: 85–210 points) survival predictions.

Survival analysis based on key predictors

Kaplan-Meier analyses were performed to evaluate the survival differences stratified by key predictors identified in the nomogram. For continuous variables (Fig. 6), optimal cutoff values were determined using maximally selected rank statistics (Supplementary Table 6). QRS duration (cutoff: 102 ms, $p = 0.011$), age (cutoff: 71.1 years, $p < 0.0001$), and NT-proBNP (cutoff: 3,833 pg/mL, $p < 0.0001$) demonstrated significant stratification of survival outcomes, while T wave offset (cutoff: 400 ms) showed a non-significant trend ($p = 0.12$). For categorical variables (Supplementary Fig. 6), NYHA functional classification demonstrated the strongest prognostic stratification ($p < 0.0001$), with the number at risk decreasing from 155, 216, and 74 at baseline to 98, 123, and 30 at 4 years for classes II, III, and IV, respectively. Left ventricular systolic dysfunction was significantly associated with survival ($p = 0.005$), with worse outcomes in the dysfunction group ($n = 32$) compared to those without dysfunction ($n = 280$). Aortic valve annulus calcification showed strong prognostic value ($p = 0.00051$), with notably worse survival in patients with calcification ($n = 20$) versus without ($n = 292$). Atrial septal defect showed a marginal association with survival ($p = 0.087$), though interpretation was limited by the small number of cases

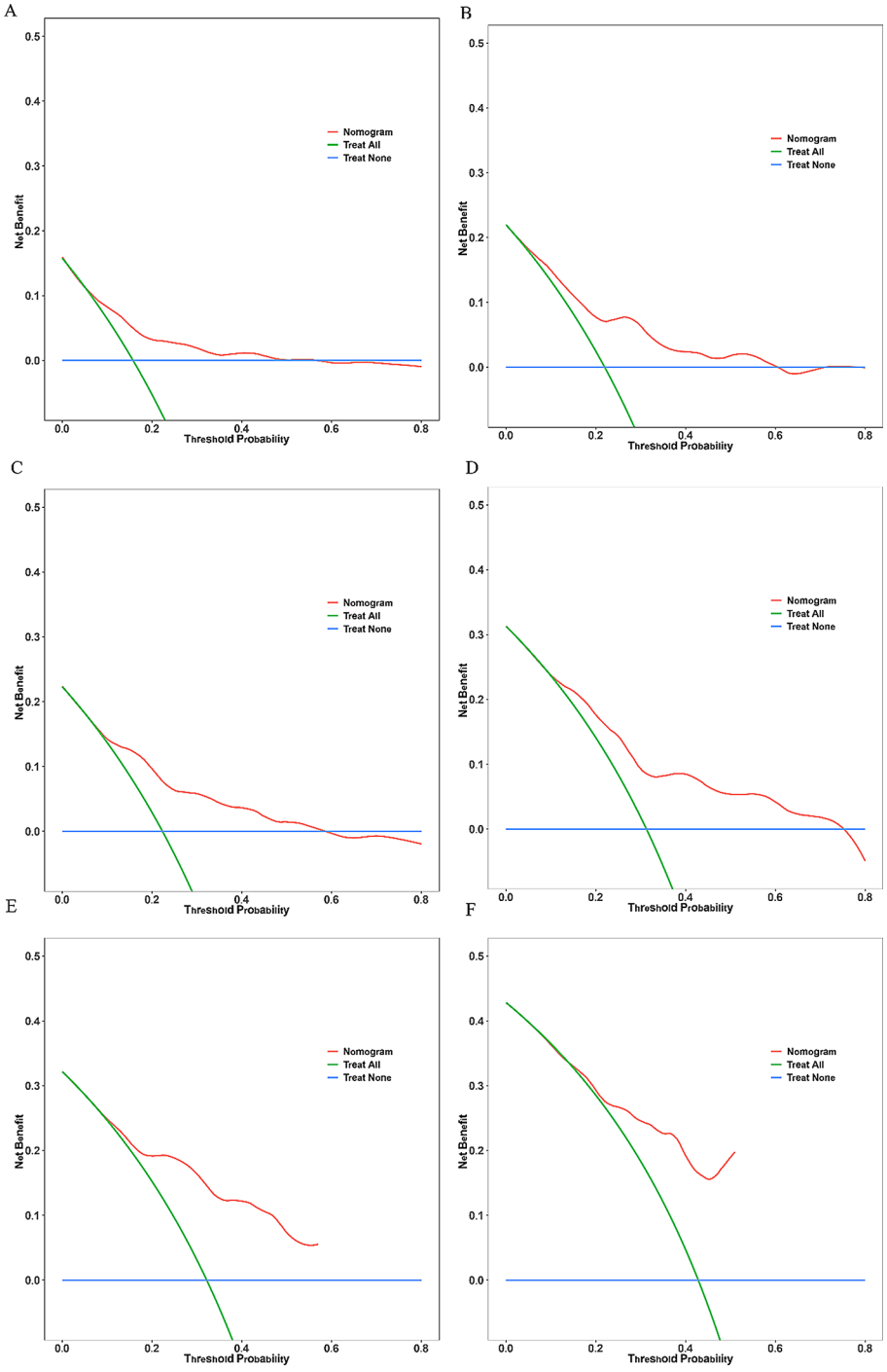

Fig. 4 Decision Curve Analysis for the Prediction Model. Decision curves for 2-year (**A**, **B**), 3-year (**C**, **D**), and 5-year (**E**, **F**) mortality prediction in the training (**A**, **C**, **E**) and validation (**B**, **D**, **F**) cohorts. The x-axis shows the threshold probability, and the y-axis shows the net benefit. Red line represents the nomogram, green line represents treating all patients, and blue line represents treating no patients

($n = 3$). Tricuspid regurgitation severity also demonstrated significant survival differences across no ($n = 76$), mild ($n = 182$), moderate ($n = 40$), and severe ($n = 14$) grades ($p = 0.0085$). Statistical details regarding the optimal cutoff values and their corresponding test statistics are provided in Supplementary Table 6. For the survival analysis of 9 variables, only NT-proBNP had missing values. We have added the survival curves for the original data in Supplementary Fig. 7, and the conclusions drawn from both the original and imputed data are consistent.

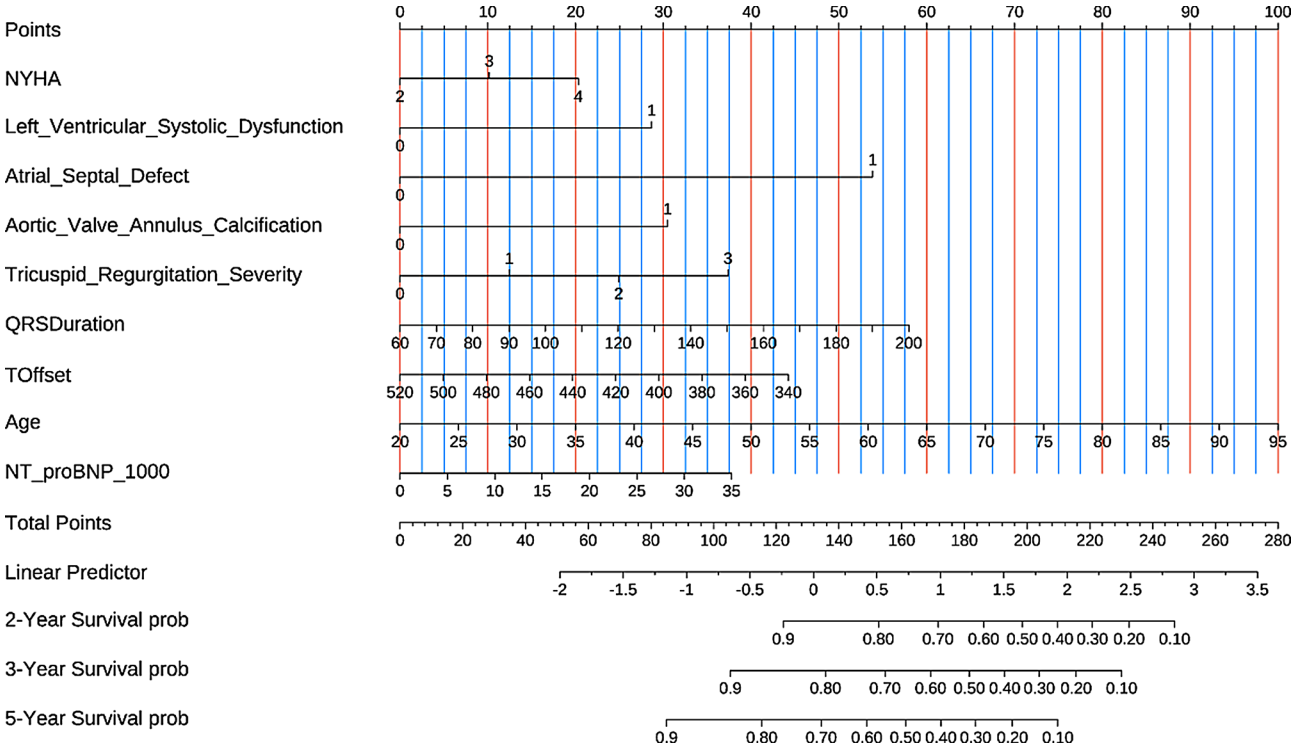

Fig. 5 Nomogram for Predicting 2-, 3-, and 5-year Survival Probabilities in Heart Failure Patients. NYHA: 2: II; 3: III; 4: IV. Atrial septal defect: 0: No;1: Yes. Aortic valve annulus calcification: 0: No;1: Yes Abbreviation: NYHA: New York Heart Association; NT-proBNP: N-terminal pro-brain natriuretic peptide

Nonlinear association analysis

To explore the complex relationships between continuous predictors and mortality risk, we performed restricted cubic spline analyses both in the main model (Fig. 7) and with covariate adjustment (Supplementary Fig. 8). For each continuous variable, we adjusted for the other eight significant predictors identified in the multivariate Cox regression analysis, excluding the variable under investigation. In the adjusted analysis, NT-proBNP maintained a significant non-linear association with mortality (P for overall < 0.001, P for non-linear < 0.001), characterized by a steep increase in hazard ratio up to 15,000 pg/mL followed by a plateau and slight decline. Age similarly demonstrated robust association with mortality (P for overall < 0.001) and marginally significant non-linearity (P for non-linear = 0.059), showing a relatively stable risk until age 60 years followed by an exponential increase. QRS duration exhibited a modest linear trend without statistical significance (P for overall = 0.213, P for non-linear = 0.605), while T wave offset showed no significant association with mortality (P for overall = 0.857, P for non-linear = 0.721) after covariate adjustment. These patterns remained consistent in both unadjusted and adjusted analyses, suggesting the robustness of these relationships independent of other significant clinical predictors.

Random survival forest analysis

To assess variable importance and compare with the Cox model, we constructed a random survival forest model using the training cohort. The optimal model parameters were determined through iterative testing of node sizes ranging from 1 to 75 (Supplementary Table 8). Using 1000 trees and an optimal node size of 7, the model achieved an out-of-bag error rate of 31.76%. Variable importance analysis revealed age and NT-proBNP as the strongest predictors, followed by QRS duration and clinical parameters including tricuspid regurgitation severity, NYHA class, and cardiac structural abnormalities (Fig. 8). The error rate stabilized after approximately 400 trees (Supplementary Fig. 9), suggesting adequate model convergence (Figs. 9 and 10).

Model comparison across different time horizons

Comprehensive model comparisons were performed for 2-, 3-, and 5-year mortality predictions. The following models were used for mortality prediction: Model A: NYHA + Left ventricular systolic dysfunction + Atrial septal defect + Aortic valve annulus calcification + Tricuspid regurgitation severity + QRS Duration + T Offset + Age + NT-ProBNP/1000; Model B: Age; Model C: NT-ProBNP/1000; Model D: QRS Duration;

Model E: Tricuspid regurgitation severity; Model F: NYHA. For 2-year prediction in the training cohort, Model A (incorporating all nine variables) showed

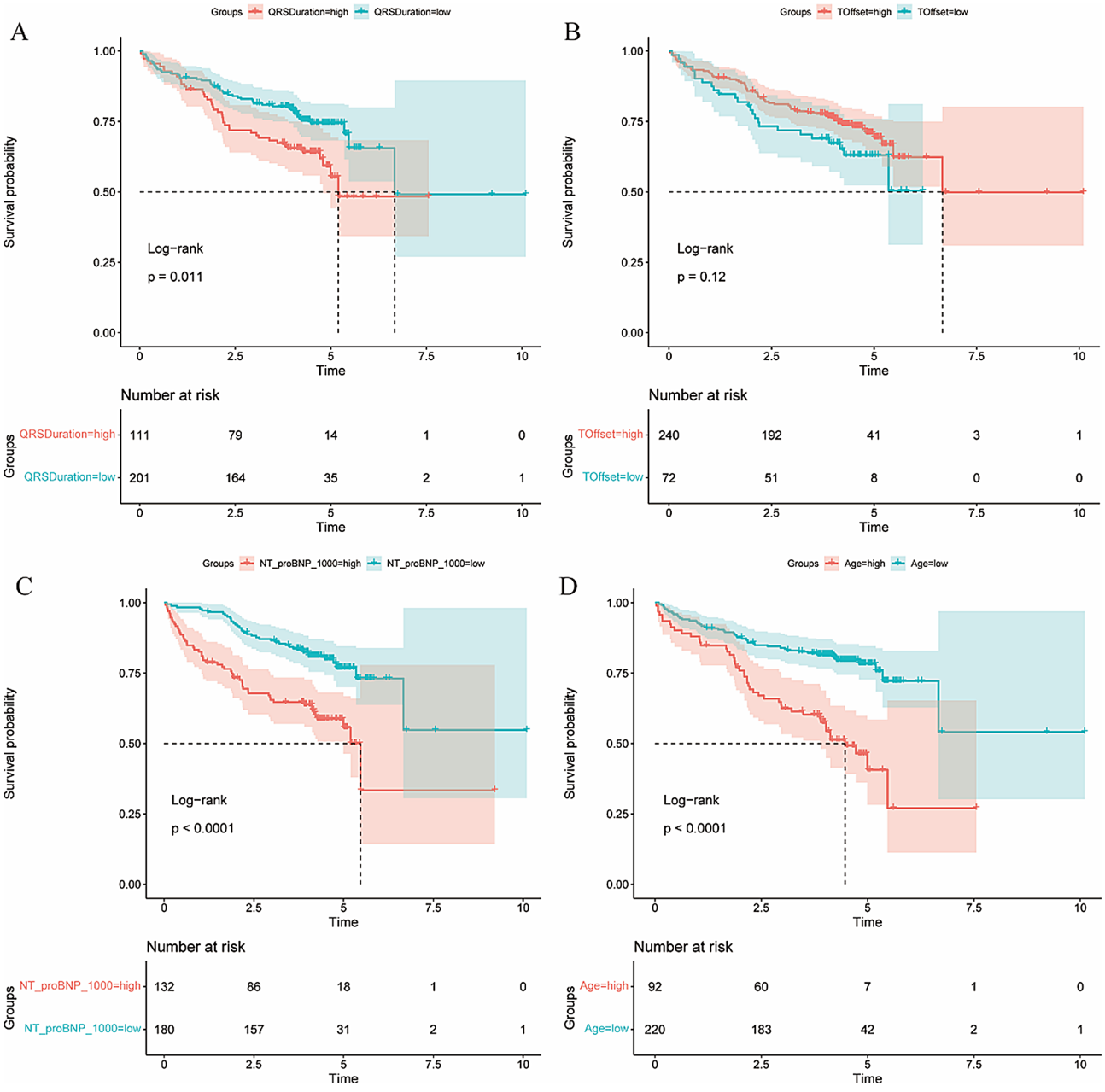

Fig. 6 Kaplan-Meier Survival Curves for Continuous Variables in the Final Model. (**A**) QRS duration stratified by cutoff value of 102 ms. high:>102ms; low: ≤102ms. (**B**) T wave offset stratified by cutoff value of 400 ms. high:>400ms; low: ≤400ms. (**C**) NT-proBNP stratified by cutoff value of 3,833 pg/mL. high:>3,833 pg/mL; low: ≤3,833 pg/mL. (**D**) Age stratified by cutoff value of 71.1 years. high:>71.1 years; low: ≤71.1 years Abbreviation: NT-proBNP: N-terminal pro-brain natriuretic peptide

superior discrimination (AUC = 0.726, 95% CI: 0.648–0.805) compared to single-predictor models, with Models B (AUC = 0.600, 95% CI: 0.509–0.691) and C (AUC = 0.685, 95% CI: 0.608–0.763) showing moderate performance. The discriminative ability improved for 3-year prediction, with Model A achieving an AUC of 0.755 (95% CI: 0.691–0.820), and further increased for 5-year prediction (AUC = 0.809, 95% CI: 0.737–0.881). In the validation cohort, Model A maintained stable performance across all time points (2-year: AUC = 0.686, 95% CI: 0.585–0.787; 3-year: AUC = 0.678, 95% CI: 0.582–0.774; 5-year: AUC = 0.706, 95% CI: 0.547–0.866). Notably, Model B (age alone) showed comparable or slightly better performance in the validation cohort for longer time horizons (3-year: AUC = 0.694, 95% CI: 0.598–0.789; 5-year: AUC = 0.723, 95% CI: 0.576–0.871) (Supplementary Figs. 8–11, Figs. 11 and 12).Calibration plots demonstrated good agreement between predicted and observed

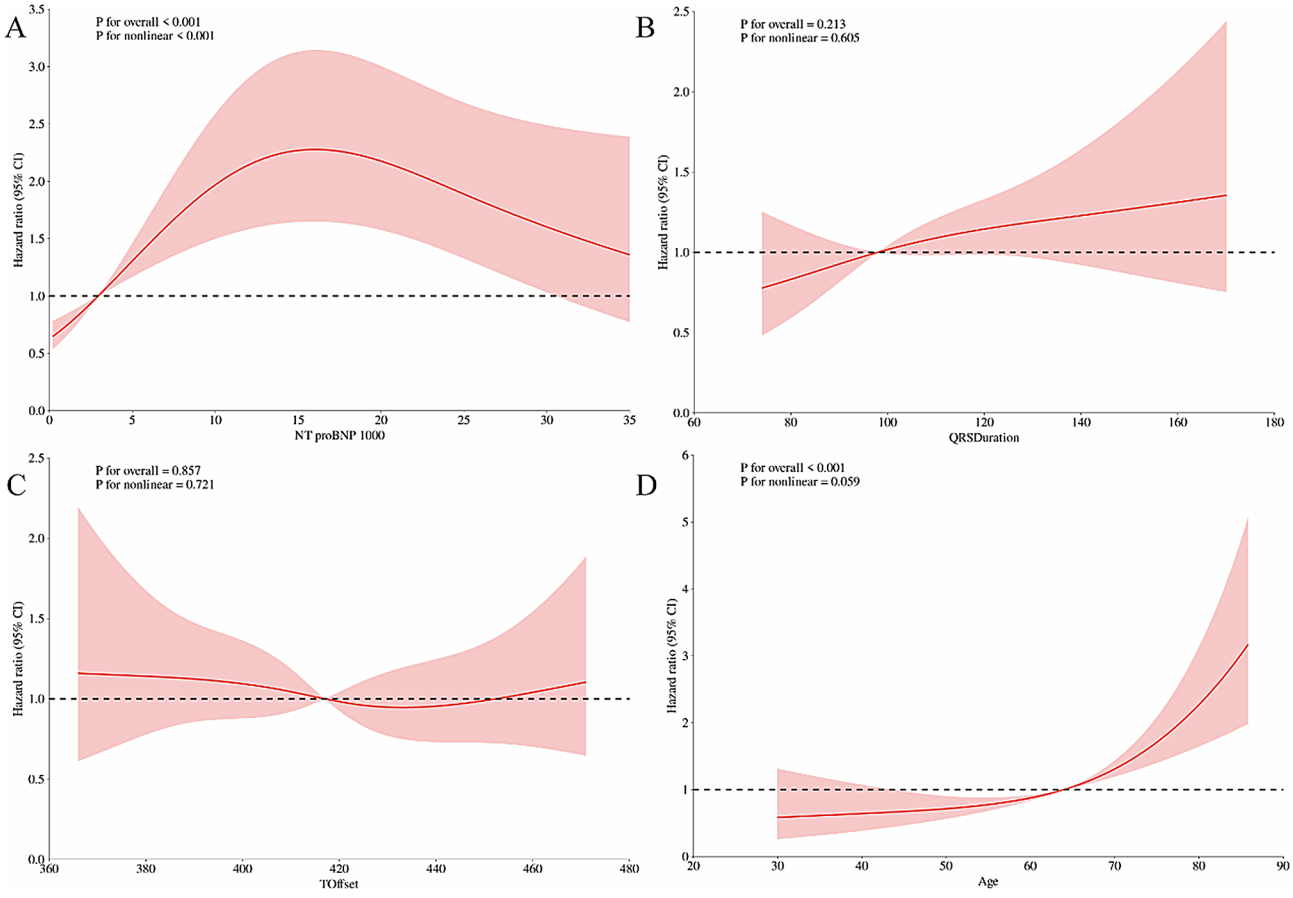

Fig. 7 Unadjusted Restricted Cubic Spline Analysis of Continuous Variables and Mortality Risk. (**A**) NT-proBNP level. (**B**) QRS duration. (**C**) T wave offset. (**D**) Age. Red lines represent hazard ratios and pink shaded areas represent 95% confidence intervals

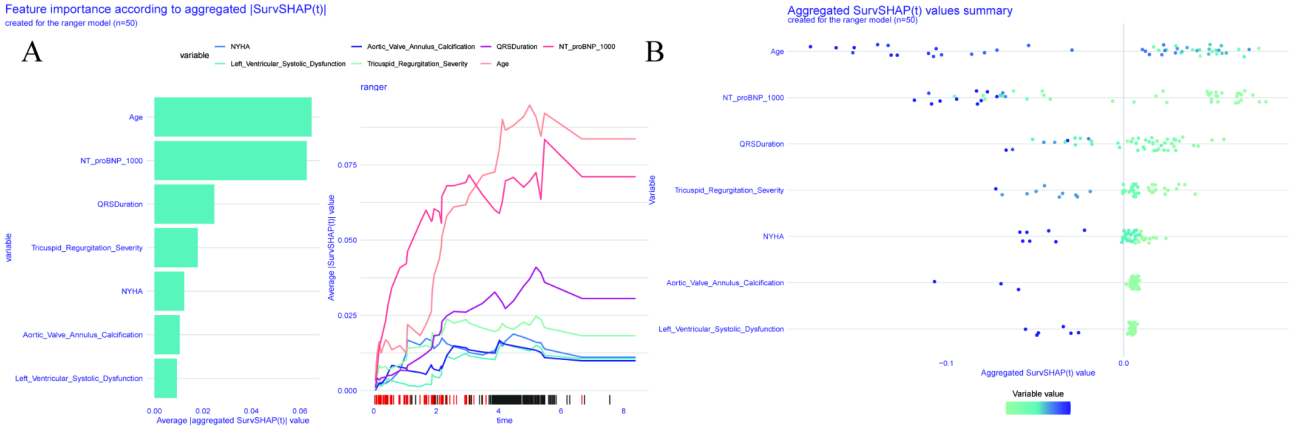

Fig. 8 Variable Importance Analysis from Random Survival Forest Model. (**A**) Feature importance according to aggregated SurvSHAP(t) values. (**B**) Distribution of aggregated SurvSHAP(t) values across different variable levels

probabilities across all time points, particularly for Models A and B. Decision curve analyses consistently showed that Model A provided superior net benefit across a wider range of threshold probabilities compared to simplified models and default strategies, with this advantage being most pronounced in 5-year predictions.

Discussion

In this comprehensive study of heart failure prognosis, we developed and validated a multimodal prediction model integrating demographic characteristics, ECG parameters, echocardiographic measurements, NT-proBNP levels, and NYHA classification. Our model demonstrated

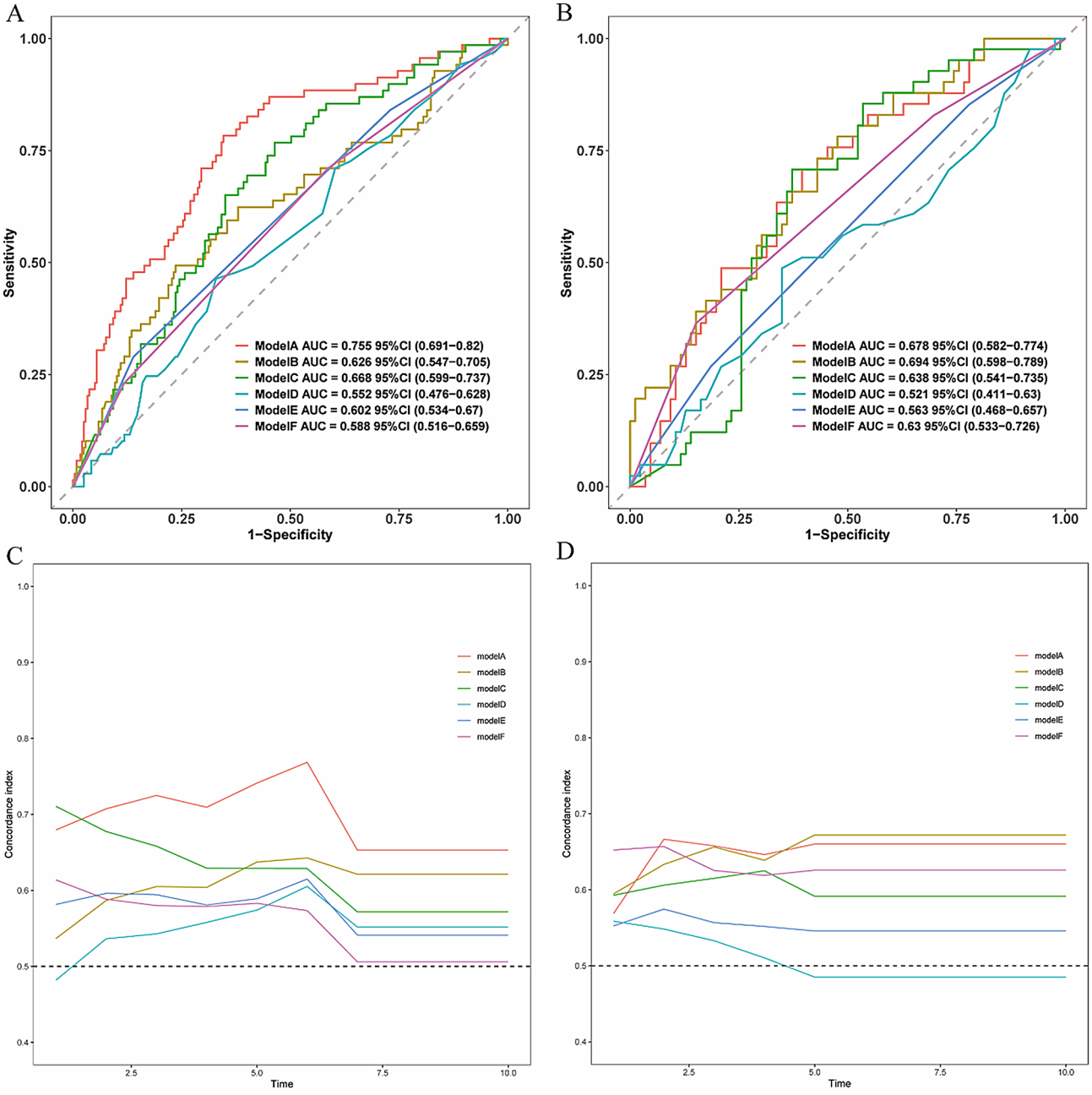

Fig. 9 Discriminative Performance of Different Models for 3-Year Mortality Prediction. Model A: NYHA + Left ventricular systolic dysfunction + Atrial septal defect + Aortic valve annulus calcification + Tricuspid regurgitation severity + QRS Duration + T Offset + Age + NT-ProBNP/ 1000; Model B: Age; Model C: NT-ProBNP/ 1000; Model D: QRS Duration; Model E: Tricuspid regurgitation severity; Model F: NYHA

robust predictive performance with C-indices of 0.720 (95% CI: 0.665–0.775) in the training cohort and 0.649 (95% CI: 0.569–0.729) in the validation cohort. Notably, the model showed excellent discrimination for 5-year mortality (AUC = 0.809, 95% CI: 0.737–0.881) and maintained consistent calibration across different time points. In a similar study, Lin et al. developed a predictive model for all-cause mortality in patients with coexisting HF and atrial fibrillation [24]. This model identified eight key predictors: age, sex, New York Heart Association (NYHA) heart function class III or IV, history of myocardial infarction, and levels of albumin, triglycerides, N-terminal pro-B-type natriuretic peptide, and blood urea nitrogen. This is broadly similar to the risk factors we selected. Furthermore, in another study, a prognostic score integrating remotely recorded heart failure symptoms and clinical risk factors was developed and validated to predict mortality risk after myocardial infarction. The study found that combining heart failure symptoms with clinical variables provides better risk stratification than the

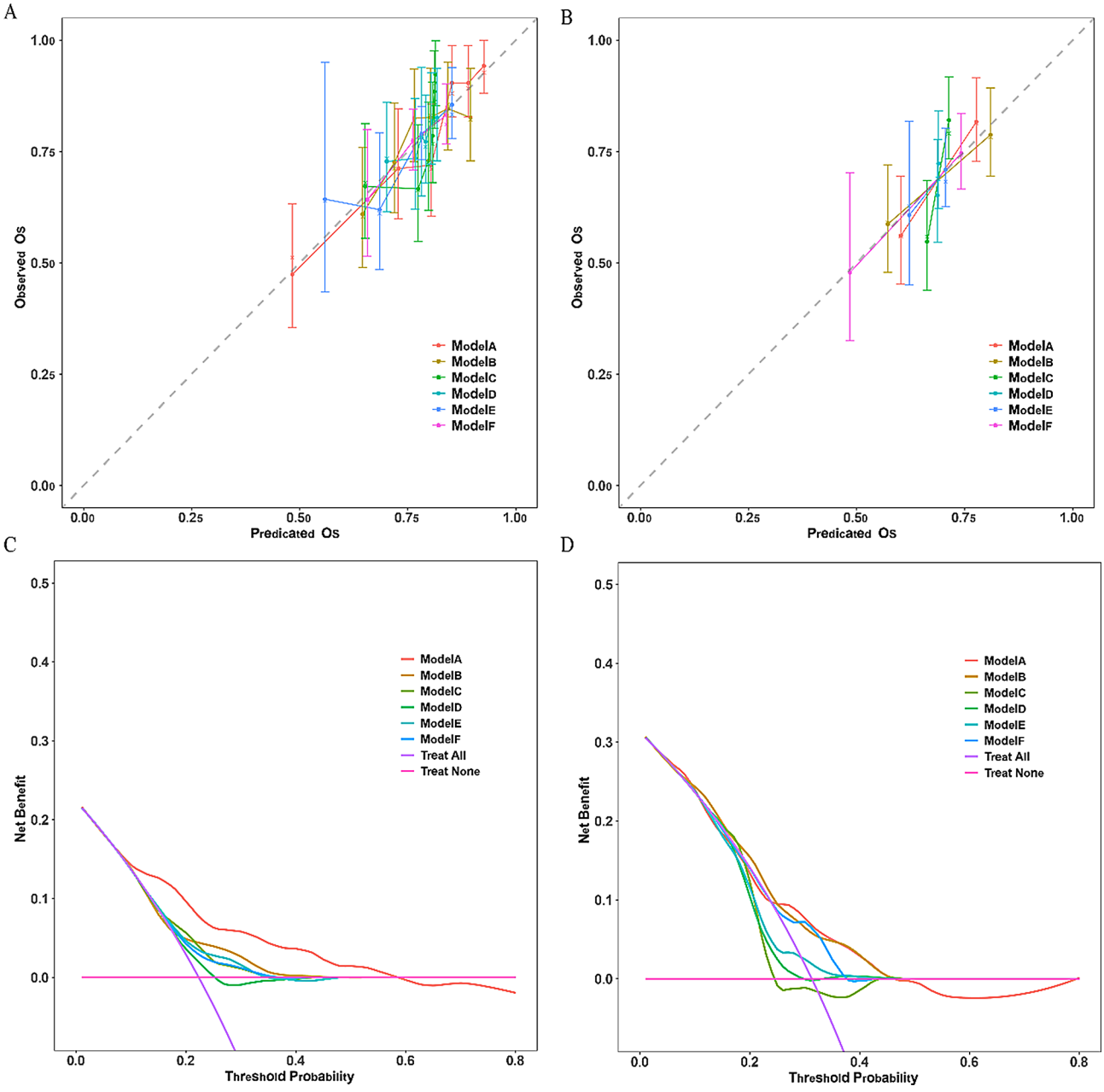

Fig. 10 Calibration and Clinical Utility of Different Models for 3-Year Mortality Prediction. Model A: NYHA + Left ventricular systolic dysfunction + atrial septal defect + Aortic valve annulus calcification + Tricuspid regurgitation severity + QRS Duration + T Offset + Age + NT-ProBNP/ 1000; Model B: Age; Model C: NT-ProBNP/ 1000; Model D: QRS Duration; Model E: Tricuspid regurgitation severity; Model F: NYHA

currently proposed GRACE score [25]. These studies emphasize the importance of integrating various clinical parameters to develop prognostic models that can aid in the management of heart failure patients.

Relationship between age and mortality risk

This study highlights that age is a significant predictor of mortality in HF patients, demonstrating a marked nonlinear relationship, particularly after the age of 60, where the risk of death increases rapidly. This phenomenon reflects the pathophysiological changes occurring during cardiovascular aging, including myocardial stiffness, reduced β-adrenergic responsiveness, and impaired calcium ion influx regulation [26, 27]. With advancing age, the structural and functional degradation of the cardiovascular system progressively worsens, including arterial stiffening, increased cardiac load, and compensatory cardiac remodeling [28]. These changes, by altering the heart's pumping ability, not only increase the incidence of HF but also exacerbate its severity. Research indicates

that age-related vascular dysfunction and increased arterial stiffness are closely associated with the progression of cardiac remodeling [29]. These structural and functional alterations can accelerate the progression of HF by affecting hemodynamics, coronary blood flow, and cardiac output [30, 31]. Therefore, age is not only an independent risk factor for HF but also contributes to an accelerating increase in mortality risk as comorbidities accumulate.

Electrophysiological remodeling and heart failure progression

Electrocardiogram (ECG) parameters, especially QRS duration and T-wave characteristics, have become crucial tools in the prognostic assessment of HF patients. QRS duration reflects the electrophysiological activity of the heart's surface and can be used to assess whether the ventricular myocyte depolarization process is functioning normally. In HF patients, the electrocardiogram typically shows prolonged QRS duration [32, 33]. Studies have shown that HF patients with a QRS duration < 120 ms exhibit better cardiac function compared to those with a QRS duration > 120 ms. Moreover, QRS duration is positively correlated with the left ventricular diameter [34, 35]. The results of this study indicate that for each 1-millisecond increase in QRS duration, the risk of mortality in heart failure patients increases by 1%. The mechanism underlying prolonged QRS duration in HF patients is primarily due to myocardial ischemia and ventricular remodeling, which lead to an increase in the relative surface area of myocardial cell membranes. This results in a reduction in the number of Na+/K + pumps, causing pump dysfunction. Consequently, the synchronization of cardiac mechanical activity is impaired, and the depolarization velocity of the action potential is significantly slowed, leading to a prolonged QRS duration [36]. Prolonged QRS duration is also associated with impaired atrial synchrony, which can cause cardiac hemodynamic disturbances, a decline in ejection fraction, and myocardial cell damage. This, in turn, increases the risk of myocardial fibrosis and necrosis, contributing to major adverse cardiovascular events [37]. Abnormal T-waves generally reflect disturbances in cardiac repolarization, which may be related to electrolyte imbalances or intrinsic cardiac electrophysiological alterations [38, 39]. In HF patients, T-wave abnormalities are closely associated with fatal arrhythmias such as atrial fibrillation and ventricular fibrillation, suggesting that changes in T-wave morphology could serve as early signals of electrophysiological remodeling and possess significant prognostic value [40, 41].

Structural heart disease and mortality risk

Echocardiographic parameters play a key role in the prognostic assessment of HF patients. Left ventricular systolic dysfunction, atrial septal defects, aortic valve calcification, and tricuspid regurgitation (TR) are common structural cardiac abnormalities in HF patients, particularly left ventricular systolic dysfunction. Patients with reduced ejection fraction typically have a poor prognosis [3, 42, 43]. Left ventricular dysfunction impairs the heart's pumping capacity and further increases cardiac workload through elevated intracardiac pressures, leading to cardiac dilation [44]. As the disease progresses, left ventricular remodeling and fibrosis become irreversible pathological features, significantly reducing contractile function and worsening clinical symptoms [45]. Although atrial septal defects are relatively rare, they have a significant impact on prognosis by increasing right heart load, potentially leading to right heart failure [46]. Moreover, these defects can induce hemodynamic instability, further increasing mortality risk. Therefore, early identification and correction of such structural defects are crucial for improving patient outcomes [47]. Aortic valve calcification, a common pathological feature in elderly HF patients, is closely associated with left ventricular systolic dysfunction [48]. Calcification not only increases the mechanical burden on the heart but also leads to valvular dysfunction and hemodynamic abnormalities, significantly raising mortality risk [48]. Tricuspid regurgitation (TR), a prevalent structural abnormality in HF patients, is closely related to mortality risk. Severe TR leads to right heart pressure overload and can ultimately result in right heart failure, closely linked to pulmonary hypertension caused by left heart failure [49]. TR increases the burden on the right ventricle, potentially leading to right atrial dilation and systemic venous congestion, thereby worsening HF symptoms and significantly reducing survival rates [50]. Therefore, the assessment and management of TR should be of critical importance in clinical practice.

NT-proBNP and heart failure prognosis

NT-proBNP, a cardiac biomarker, has been widely utilized for the diagnosis and prognostic evaluation of HF. Studies indicate a non-linear relationship between NT-proBNP levels and mortality risk, with a significant increase in mortality risk when NT-proBNP concentrations exceed 3000 pg/mL [51]. This finding is consistent with existing literature and suggests that elevated NT-proBNP levels are closely related to the severity of cardiac pressure overload and dysfunction [52]. NT-proBNP reflects not only cardiac pressure load but also cardiac dilation, fibrosis, and neurohormonal activation [53]. In long-term HF patients, increased NT-proBNP levels often signal disease progression, and its dynamic changes provide important prognostic information for clinicians [54]. Therefore, NT-proBNP holds significant clinical value in predicting mortality risk in HF patients and, when used in conjunction with other biomarkers and

imaging parameters, can significantly improve prognostic accuracy [55].

NYHA classification and clinical prognosis of heart failure

The NYHA functional classification is a standardized tool for assessing the clinical severity of HF. This study found that as the NYHA class increases, mortality risk also rises, closely reflecting worsening functional status [56, 57]. However, due to the subjective nature of the NYHA classification, interobserver variability may affect its accuracy in different clinical settings [58, 59]. Thus, combining objective cardiac function indicators, such as echocardiographic findings, NT-proBNP levels, and ECG parameters, can provide a more precise assessment of HF prognosis [60]. Although the NYHA classification is commonly used to evaluate HF severity, its limitations lie in not fully reflecting individual patient differences [61]. Therefore, comprehensive analysis and multidimensional assessment are essential for more accurate prognostication.

Application of machine learning and artificial intelligence in heart failure prognosis

In recent years, machine learning and artificial intelligence (AI) have shown immense potential in the risk prediction, early diagnosis, and personalized treatment of HF. AI technologies can analyze vast amounts of clinical data to identify complex patterns that traditional statistical methods may miss, offering new insights into early HF intervention [62, 63]. By integrating multimodal data, including biomarkers, imaging features, and ECG parameters, AI can significantly enhance the accuracy of mortality risk prediction in HF and provide a basis for personalized treatment decisions [64]. Deep learning models are increasingly used in HF prognosis, and it is anticipated that AI will play an increasingly vital role in HF management, facilitating more precise and individualized treatment approaches [65, 66]. Furthermore, AI's advantages in integrating and analyzing complex data can offer intelligent support for clinical decision-making [67, 68].

The strengths of our study include a comprehensive multimodal approach, rigorous validation, and clinically relevant timeframes. The model's excellent discrimination and calibration at different time points highlight its practical utility in both short-term and long-term risk prediction. Several limitations of our study should be noted. First, the follow-up duration was relatively short, with a median follow-up of 4.14 years. Longer follow-up periods may provide a more complete picture of the long-term prognostic performance of the model. Future studies will include extended follow-up to assess its long-term utility. Second, our cohort was derived from a single large tertiary hospital in China, which may limit the generalizability of our findings to other ethnic populations. We plan to pursue international multicenter collaborations in the future to validate the model across diverse populations. Third, the sample size of our study was relatively small, with only 445 patients included. This may affect the robustness of the model's performance, and we plan to include a larger cohort in future studies to further evaluate the model's validity. Fourth, the data used were primarily based on static features, and we did not collect laboratory test results or echocardiographic data at multiple time points during patients' hospitalization. In future studies, we plan to incorporate more longitudinal data and repeated measurements to more comprehensively assess disease progression and enhance the accuracy of the predictive model. Fifth, the absence of advanced imaging data, such as cardiac magnetic resonance imaging (CMR), is a limitation of this study. CMR provides detailed information on cardiac structure and function that could potentially improve the model's predictive accuracy. However, due to the relatively low proportion of patients who underwent CMR and the challenges in extracting imaging data, we were unable to include CMR data in this analysis. We recognize the potential benefits of incorporating such data and will consider its inclusion in future versions of the model. Lastly, while the model performed well in the validation cohort, we observed that age alone showed comparable performance to the full nomogram, particularly for longer follow-up periods. This finding highlights the continued importance of age as a key prognostic factor in the long-term management of heart failure patients.

Conclusion

This study provides a comprehensive analysis of the relationship between various clinical parameters and mortality risk in HF patients, emphasizing the critical role of indicators such as electrocardiogram (ECG), echocardiography, and NT-proBNP in risk prediction. With the continued advancement in the understanding of HF pathophysiology and the application of cutting-edge technologies, there is great potential for further improving prognostic evaluation in HF patients through more precise biomarkers and artificial intelligence models. This progress is expected to facilitate the development of more personalized treatment strategies, enhancing patient outcomes in the future.

Supplementary Information

The online version contains supplementary material available at https://doi.org/10.1186/s12872-025-04642-7.

Supplementary Material 1

Supplementary Material 2

Author contributions
Yahui Li, Xujie Wang and Jiayu Xu collected the data, Xuhui Liu and Yahui Li analyzed the data and wrote the manuscript, and Kunlun He and Chunxia Zhao conceived the ideas and assisted in revising the manuscript. Yahui Li and Jiayu Xu are co-first authors and contribute equally to this work. All the authors reviewed the manuscript.

Funding
This research did not receive any specific grant from funding agencies in the public, commercial, or not-for-profit sectors.

Data availability
The datasets used and/or analyzed during the current study are available from the corresponding author on reasonable request.

Declarations

Ethical approval
The study was approved by the First Medical Center of People's Liberation Army General Hospital (S2022-203-02). This research study was reviewed and approved by the Ethics Committee at Hospital, waiving the requirement for informed consent in alignment with the Declaration of Helsinki.

Competing interests
The authors declare no competing interests.

Author details
[1]Division of Cardiology, Department of Internal Medicine, Tongji Hospital, Tongji Medical College, Hubei Key Laboratory of Genetics and Molecular Mechanisms of Cardiological Disorders, Huazhong University of Science and Technology, 1095 Jiefang Ave, Wuhan, Hubei 430030, China
[2]First Medical Center of People's Liberation Army General Hospital, Beijing 100853, China
[3]Department of Neurology, The Second Hospital of Lanzhou University, 82 Chenyimen, Chengguan District, Lanzhou, Gansu 730030, China
[4]Department of Emergency ICU, The Affiliated Hospital of Qinghai University, Xining, China
[5]Medical Innovation Research Division of People's Liberation Army General Hospital, Beijing 100853, China

Received: 3 February 2025 / Accepted: 7 March 2025
Published online: 26 March 2025

References

1. Ziaeian B, Fonarow GC. Epidemiology and aetiology of heart failure. Nat Rev Cardiol. 2016;13:368–78.
2. Mensah GA, Roth GA, Fuster V. The global burden of cardiovascular diseases and risk factors: 2020 and beyond. J Am Coll Cardiol. 2019;74:2529–32.
3. Aşkin L, Tanriverđi O. The benefits of Sacubitril-Valsartan in low ejection fraction heart failure. Bolu Abant Izzet Baysal Univ Tip Fak Abant Tip Derg. 2022;11:337–336.
4. Zhang Y, Wang H, Yin C, Shu T, Yu J, Jian J, et al. Development of a prediction model for the risk of 30-day unplanned readmission in older patients with heart failure: A multicenter retrospective study. Nutr Metab Cardiovasc Dis NMCD. 2023;33:1878–87.
5. Khera R, Pandey A, Ayers CR, Agusala V, Pruitt SL, Halm EA, et al. Contemporary epidemiology of heart failure in Fee-For-Service medicare beneficiaries across healthcare settings. Circ Heart Fail. 2017;10:e004402.
6. Taylor CJ, Ordóñez-Mena JM, Roalfe AK, Lay-Flurrie S, Jones NR, Marshall T, et al. Trends in survival after a diagnosis of heart failure in the united Kingdom 2000–2017: population based cohort study. BMJ. 2019;364:l223.
7. McDonagh TA, Metra M, Adamo M, Gardner RS, Baumbach A, Böhm M, et al. 2021 ESC guidelines for the diagnosis and treatment of acute and chronic heart failure. Eur Heart J. 2021;42:3599–726.
8. Heidenreich PA, Bozkurt B, Aguilar D, Allen LA, Byun JJ, Colvin MM, et al. 2022 AHA/ACC/HFSA guideline for the management of heart failure: A report of the American college of cardiology/american heart association joint committee on clinical practice guidelines. Circulation. 2022;145:e895–1032.
9. Elendu C, Amaechi DC, Elendu TC, Fiemotonghan B-E, Okoye OK, Agu-Ben CM, et al. A comprehensive review of heart failure: unraveling the etiology, decoding pathophysiological mechanisms, navigating diagnostic modalities, exploring Pharmacological interventions, advocating lifestyle modifications, and charting the horizon of emerging therapies in the complex landscape of chronic cardiac dysfunction. Med (Baltim). 2024;103:e36895.
10. Petrie MC, Lee MMY, Docherty KF. Sodium-glucose co-transporter 2 inhibitors-the first successful treatment for heart failure with preserved ejection fraction? Eur J Heart Fail. 2021;23:1256–9.
11. Cho Y, Yoon M, Kim J, Lee JH, Oh I-Y, Lee CJ, et al. Artificial Intelligence-Based electrocardiographic biomarker for outcome prediction in patients with acute heart failure: prospective cohort study. J Med Internet Res. 2024;26:e52139.
12. Moneghetti KJ, Singh T, Hedman K, Christle JW, Kooreman Z, Kobayashi Y, et al. Echocardiographic assessment of left ventricular remodeling in American style footballers. Int J Sports Med. 2020;41:27–35.
13. Prana Jagannatha GN, Suastika LOS, Kosasih AM, de Liyis BG, Yusrika MU, Kamardi S, et al. Prognostic value of baseline echocardiographic parameters in heart failure with improved vs nonrecovered ejection fraction. CJC Open. 2023;5:859–69.
14. Zdebik N, Poręba R, Gać P. Importance of T1-Mapping sequence in patients with hypertrophic cardiomyopathy without foci of Non-Ischemic myocardial injury in late gadolinium enhancement sequence. Biomedicines. 2024;12:1330.
15. Vergaro G, Gentile F, Meems LMG, Aimo A, Januzzi JL, Richards AM, et al. NT-proBNP for risk prediction in heart failure: identification of optimal cutoffs across body mass index categories. JACC Heart Fail. 2021;9:653–63.
16. Brouwers FP, van Gilst WH, Damman K, van den Berg MP, Gansevoort RT, Bakker SJL, et al. Clinical risk stratification optimizes value of biomarkers to predict new-onset heart failure in a community-based cohort. Circ Heart Fail. 2014;7:723–31.
17. Singh G, Bamba H, Inban P, Chandrasekaran SH, Priyatha V, John J, et al. The role of biomarkers in the prognosis and risk stratification in heart failure: A systematic review. Dis–Mon DM. 2024;70:101782.
18. Xu Z, Hu Y, Shao X, Shi T, Yang J, Wan Q, et al. The efficacy of machine learning models for predicting the prognosis of heart failure: A systematic review and Meta-Analysis. Cardiology. 2025;150:79–97.
19. Dhingra LS, Aminorroaya A, Sangha V, Camargos AP, Asselbergs FW, Brant LC et al. Scalable risk stratification for heart failure using artificial intelligence applied to 12-lead electrocardiographic images: A multinational study. MedRxiv Prepr Serv Health Sci. 2024;:2024.04.02.24305232.
20. Frizzell JD, Liang L, Schulte PJ, Yancy CW, Heidenreich PA, Hernandez AF, et al. Prediction of 30-Day All-Cause readmissions in patients hospitalized for heart failure: comparison of machine learning and other statistical approaches. JAMA Cardiol. 2017;2:204–9.
21. Zhang Y, Xiang T, Wang Y, Shu T, Yin C, Li H, et al. Explainable machine learning for predicting 30-day readmission in acute heart failure patients. iScience. 2024;27:110281.
22. Smole T, Žunkovič B, Pičulin M, Kokalj E, Robnik-Šikonja M, Kukar M, et al. A machine learning-based risk stratification model for ventricular tachycardia and heart failure in hypertrophic cardiomyopathy. Comput Biol Med. 2021;135:104648.
23. Zhao Q-Y, Wang H, Luo J-C, Luo M-H, Liu L-P, Yu S-J, et al. Development and validation of a Machine-Learning model for prediction of extubation failure in intensive care units. Front Med. 2021;8:676343.
24. Guan L, Wang C-H, Sun H, Sun Z-J. Development and validation of a nomogram model for all-cause mortality risk in patients with chronic heart failure and atrial fibrillation. BMC Geriatr. 2024;24:470.
25. Wohlfahrt P, Jenča D, Melenovský V, Stehlik J, Mrázková J, Šramko M, et al. Development and validation of a prognostic score integrating remote heart failure symptoms and clinical variables in mortality risk prediction after myocardial infarction: the PragueMi score. Eur J Prev Cardiol. 2024;31:1713–20.
26. Großkopf A, Saemann L, Szabó G, Simm A. [Biological mechanisms of aging in the cardiovascular system]. Z Gerontol Geriatr. 2022;55:455–60.
27. Zhao R, Yan Y, Dong Y, Wang X, Li X, Qiao R, et al. FGF13 deficiency ameliorates calcium signaling abnormality in heart failure by regulating microtubule stability. Biochem Pharmacol. 2024;225:116329.
28. Athyros VG, Pagourelias ED, Gossios TD, Vasilikos VG. Treating heart failure with preserved ejection fraction related to arterial stiffness. Can we kill two birds with one stone?? Curr Vasc Pharmacol. 2015;13:368–80.

29. Fang Z, Raza U, Song J, Lu J, Yao S, Liu X, et al. Systemic aging fuels heart failure: molecular mechanisms and therapeutic avenues. ESC Heart Fail. 2024. https://doi.org/10.1002/ehf2.14947.
30. Nuclear remodeling drives. age-related cardiac dysfunction. Nat Aging. 2023;3:15–6.
31. Chen B, Guo J, Ye H, Wang X, Feng Y. Role and molecular mechanisms of SGLT2 inhibitors in pathological cardiac remodeling (Review). Mol Med Rep. 2024;29:73.
32. Ovchinnikov AG, Arefieva TI, Potekhina AV, Filatova AY, Ageev FT, Boytsov SA. The molecular and cellular mechanisms associated with a microvascular inflammation in the pathogenesis of heart failure with preserved ejection fraction. Acta Naturae. 2020;12:40–51.
33. Ueland T, Gullestad L, Nymo SH, Yndestad A, Aukrust P, Askevold ET. Inflammatory cytokines as biomarkers in heart failure. Clin Chim Acta Int J Clin Chem. 2015;443:71–7.
34. Aboonabi A, McCauley MD. Myofilament dysfunction in diastolic heart failure. Heart Fail Rev. 2024;29:79–93.
35. Desai AS, Solomon SD, Shah AM, Claggett BL, Fang JC, Izzo J, et al. Effect of Sacubitril-Valsartan vs Enalapril on aortic stiffness in patients with heart failure and reduced ejection fraction: A randomized clinical trial. JAMA. 2019;322:1077–84.
36. Bosch RF, Grammer JB, Kühlkamp V, Seipel L. [Electrical remodeling in atrial fibrillation–cellular and molecular mechanisms]. Z Kardiol. 2000;89:795–802.
37. Kelly JP, Daubert JP. Prolonged QRS in heart failure with preserved ejection fraction: risk marker and therapeutic target?? JACC Heart Fail. 2016;4:487–9.
38. Sun Y, Chen X, Zhang Y, Yu Y, Zhang X, Si J, et al. Reverse atrial remodeling in heart failure with recovered ejection fraction. J Am Heart Assoc. 2023;12:e026891.
39. Vermeulen JT. Mechanisms of arrhythmias in heart failure. J Cardiovasc Electrophysiol. 1998;9:208–21.
40. Kaufmann DK, Raczak G, Szwoch M, Wabich E, Świątczak M, Daniłowicz-Szymanowicz L. Baroreflex sensitivity but not microvolt T-wave alternans can predict major adverse cardiac events in ischemic heart failure. Cardiol J. 2022;29:1004–12.
41. Salerno-Uriarte JA, De Ferrari GM, Klersy C, Pedretti RFE, Tritto M, Sallusti L, et al. Prognostic value of T-wave alternans in patients with heart failure due to nonischemic cardiomyopathy: results of the ALPHA study. J Am Coll Cardiol. 2007;50:1896–904.
42. Fu K, Yang Z, Wang N, Dong Y, Wang Z, Chen W, et al. Recurrence of left ventricular systolic dysfunction and its risk factors in heart failure with improved ejection fraction patients receiving guideline-directed medical therapy: A trajectory analysis based on echocardiography. Int J Cardiol. 2024;415:132370.
43. Nishihara T, Takaya Y, Nakayama R, Yoshida Y, Toh N, Miyoshi T, et al. Prognostic value of right atrial function in patients with significant tricuspid regurgitation. ESC Heart Fail. 2024;11:4019–27.
44. Yancy CW, Jessup M, Bozkurt B, Butler J, Casey DE, Colvin MM, et al. 2017 ACC/AHA/HFSA focused update of the 2013 ACCF/AHA guideline for the management of heart failure: A report of the American college of cardiology/american heart association task force on clinical practice guidelines and the heart failure society of America. J Am Coll Cardiol. 2017;70:776–803.
45. Frantz S, Hundertmark MJ, Schulz-Menger J, Bengel FM, Bauersachs J. Left ventricular remodelling post-myocardial infarction: pathophysiology, imaging, and novel therapies. Eur Heart J. 2022;43:2549–61.
46. Upadhya B, Kitzman DW. Heart failure with preserved ejection fraction: new approaches to diagnosis and management. Clin Cardiol. 2020;43:145–55.
47. Hart EA, Zwart K, Teske AJ, Voskuil M, Stella PR, Chamuleau SaJ, et al. Haemodynamic and functional consequences of the iatrogenic atrial septal defect following Mitraclip therapy. Neth Heart J Mon J Neth Soc Cardiol Neth Heart Found. 2017;25:137–42.
48. Otto CM. Valvular aortic stenosis: disease severity and timing of intervention. J Am Coll Cardiol. 2006;47:2141–51.
49. Agricola E, Marini C, Stella S, Monello A, Fisicaro A, Tufaro V, et al. Effects of functional tricuspid regurgitation on renal function and long-term prognosis in patients with heart failure. J Cardiovasc Med Hagerstown Md. 2017;18:60–8.
50. Hahn RT, Brener MI, Cox ZL, Pinney S, Lindenfeld J. Tricuspid regurgitation management for heart failure. JACC Heart Fail. 2023;11(8 Pt 2):1084–102.
51. Jia X, Al Rifai M, Hoogeveen R, Echouffo-Tcheugui JB, Shah AM, Ndumele CE, et al. Association of Long-term change in N-Terminal Pro-B-Type natriuretic peptide with incident heart failure and death. JAMA Cardiol. 2023;8:222–30.
52. Zhang H, Li X, Zhang N, Tian L. Effect of thyroid dysfunction on N-terminal pro-B-type natriuretic peptide levels: A systematic review and meta-analysis. Front Endocrinol. 2023;14:1083171.
53. Maries L, Manitiu I. Diagnostic and prognostic values of B-type natriuretic peptides (BNP) and N-terminal fragment brain natriuretic peptides (NT-pro-BNP). Cardiovasc J Afr. 2013;24:286–9.
54. Wang Y, Fu L, Jia Q, Yu H, Zhang P, Zhang C, et al. Analyzing dynamic changes of laboratory indexes in patients with acute heart failure based on retrospective study. BioMed Res Int. 2016;2016:7496061.
55. van der Velde AR, Meijers WC, de Boer RA. Biomarkers for risk prediction in acute decompensated heart failure. Curr Heart Fail Rep. 2014;11:246–59.
56. Eltayeb M, Squire I, Sze S. Biomarkers in heart failure: a focus on natriuretic peptides. Heart Br Card Soc. 2024;110:809–18.
57. Nagai T, Anzai T. [NYHA functional classification and AHA/ACC stages for heart failure management]. Nihon Rinsho Jpn J Clin Med. 2016;74(Suppl 6):340–4.
58. Blacher M, Zimerman A, Engster PHB, Grespan E, Polanczyk CA, Rover MM, et al. Revisiting heart failure assessment based on objective measures in NYHA functional classes I and II. Heart Br Card Soc. 2021;107:1487–92.
59. Schou M, Petrie MC, Borlaug BA, Butler J, Davies MJ, Kitzman DW, et al. Semaglutide and NYHA functional class in Obesity-Related heart failure with preserved ejection fraction: the STEP-HFpEF program. J Am Coll Cardiol. 2024;84:247–57.
60. Elis A, Giladi E, Raiyan A, Atamna A. Congestive heart failure at the department of medicine: demographic and clinical characteristics. Isr Med Assoc J IMAJ. 2023;25:622–6.
61. Webb J, Jackson T, Claridge S, Sammut E, Behar J, Carr-White G. Management of heart failure with preserved ejection fraction. Practitioner. 2015;259:21–4.
62. Wang Z, Gu Y, Huang L, Liu S, Chen Q, Yang Y, et al. Construction of machine learning diagnostic models for cardiovascular pan-disease based on blood routine and biochemical detection data. Cardiovasc Diabetol. 2024;23:351.
63. Yasmin F, Shah SMI, Naeem A, Shujauddin SM, Jabeen A, Kazmi S, et al. Artificial intelligence in the diagnosis and detection of heart failure: the past, present, and future. Rev Cardiovasc Med. 2021;22:1095–113.
64. Jia H, Liao S, Zhu X, Liu W, Xu Y, Ge R, et al. Deep learning prediction of survival in patients with heart failure using chest radiographs. Int J Cardiovasc Imaging. 2024;40:1891–901.
65. Dhingra LS, Aminorroaya A, Pedroso AF, Khunte A, Sangha V, McIntyre D et al. Artificial intelligence enabled prediction of heart failure risk from Single-lead electrocardiograms. MedRxiv Prepr Serv Health Sci. 2024;:2024.05.27.24307952.
66. Kaur D, Hughes JW, Rogers AJ, Kang G, Narayan SM, Ashley EA, et al. Race, sex, and age disparities in the performance of ECG deep learning models predicting heart failure. Circ Heart Fail. 2024;17:e010879.
67. Sabouri M, Rajabi AB, Hajianfar G, Gharibi O, Mohebi M, Avval AH, et al. Machine learning based readmission and mortality prediction in heart failure patients. Sci Rep. 2023;13:18671.
68. Sideris K, Weir CR, Schmalfuss C, Hanson H, Pipke M, Tseng P-H, et al. Artificial intelligence predictive analytics in heart failure: results of the pilot phase of a pragmatic randomized clinical trial. J Am Med Inf Assoc JAMIA. 2024;31:919–28.

Publisher's note